EEET ECOLOGICAL ENGINEERING & ENVIRONMENTAL TECHNOLOGY

Ecological Engineering & Environmental Technology, 2026, 27(2), 390–416
https://doi.org/10.12912/27197050/217586
ISSN 2719–7050, License CC-BY 4.0

Received: 2025.12.30
Accepted: 2026.01.30
Published: 2026.02.07

Estimation of erosion potential and conservation planning based on universal soil loss equation model sensitivity analysis in Juwet sub-watershed, Indonesia

Nurul Hidayah[1], Slamet Suprayogi[2*], Dyah Rahmawati Hizbaron[2], Galih Dwi Jayanto[3]

[1] Master Program in Coastal Area and Watershed Management and Planning, Faculty of Geography, Universitas Gadjah Mada, Bulaksumur, Yogyakarta, 55281 Indonesia
[2] Department of Environmental Geography, Faculty of Geography, Universitas Gadjah Mada, Yogyakarta, Indonesia
[3] Center for Environmental Studies, Universitas Gadjah Mada, Yogyakarta, Indonesia
* Corresponding author's email: ssuprayogi@ugm.ac.id

ABSTRACT

Soil erosion poses a serious threat to agricultural productivity in tropical hilly areas, particularly in the Juwet Sub-Watershed with its steep slopes and intensive agricultural activities. This study aims to estimate erosion potential using USLE modeling and identify dominant factors through sensitivity analysis as a basis for conservation planning. The five USLE factors were mapped through the collection of primary and secondary data. Primary data consisted of soil samples from 19 observation points, while secondary data included rainfall data for the 2014–2023 period, SRTM 30 m, and remote sensing imagery. The one-at-a-time (OAT) method was used for sensitivity analysis to determine the contribution of each parameter to the erosion rate. The results showed that the total erosion potential reached 1,775,552 tons/year, concentrated in the middle and upper parts of the sub-watershed with a slope of 25–40%. The sensitivity results revealed that topography (LS) was the most dominant factor with a contribution of 56.71%, followed by land cover (C) at 34.66%, and conservation practices (P) at 8.33%. Temporal variation shows a pattern consistent with monthly rainfall erosivity, where the highest erosion potential occurs from November to March, peaking in November at 392,324.37 $MJ \cdot mm \cdot ha^{-1} \cdot h^{-1} \cdot month^{-1}$. More than 60% of the land has not implemented adequate conservation techniques. This quantitative dominance indicates the relative importance of topographic control on erosion dynamics in the study area. The present study enabled the identification of the dominant influence of topography on erosion processes and supports the application of sensitivity analysis as a basis for prioritizing conservation planning.

Keywords: soil erosion, tropical watershed, USLE model.

INTRODUCTION

Soil is one of the natural resources that is essential for life on Earth (Clunes et al., 2022). Its existence not only serves as medium for plant growth but also plays an important role in maintaining biodiversity, reducing the impact of climate change, protecting public health, and ensuring global food security (Hoffland et al., 2020; Keesstra et al., 2016; Or et al., 2021). Approximately 96% of the world's food needs are produced from vulnerable topsoil (Medjani et al., 2023). This condition highlights the vital role of soil for human survival and ecological systems.

However, soil erosion has become one of the most serious global environmental problems, significantly impacting the decline in topsoil fertility and agricultural productivity (Bahddou et al., 2023; Turner et al., 2018). This issue is of particular concern in watershed management (Mazigh et al., 2022; Shekar and Mathew, 2025). In mountainous areas, soil erosion is often a major threat

that has the potential to reduce land productivity, accelerate environmental degradation, and increase the risk of landslides (Teku and Derbib, 2024). Given the continuing growth of the world's population, it is crucial to understand and address the hazards associated with soil erosion. This urgency stems from the need to maintain food security, conserve water resources, and manage landscapes sustainably (Sestras et al., 2023).

Geographic information systems (GIS) can be used as an approach to analyze and map the distribution of erosion rates by integrating various spatial parameters (Javed et al., 2009; Pham et al., 2018). The use of GIS-based empirical models allows for quantitative assessment of soil loss occurring in a region. One of the most widely used models globally is the universal soil loss equation (USLE). This model is considered effective because it can estimate long-term average soil loss based on factors that cause erosion, namely rainfall erosivity (R), soil erodibility (K), slope length and steepness (LS), land cover (C), and conservation practices (P) (Ganasri and Ramesh, 2016; Mahleb et al., 2022).

This model has proven to be a practical tool for evaluating risks related to land loss and directing conservation efforts in various geographical conditions (Devatha et al., 2015; Girmay et al., 2020; Mazigh et al., 2022). As land use changes become more complex, climate patterns fluctuate, and global environmental concerns grow, the USLE model is useful in current soil conservation and land management efforts. Compared to other more complex models that require more data, USLE is commonly applied due to its simplicity, ease of implementation, and relatively easy availability of supporting data (Yadav et al., 2024). In the Indonesian context, the application of GIS-based USLE models is particularly relevant for regions with complex geographical characteristics, especially in watersheds facing high ecological pressure due to land use changes and varying rainfall intensity. This study focuses on the Juwet Sub-Watershed located in the Special Region of Yogyakarta, Indonesia.

This area has structural-denudational hills with steep slopes, making it highly susceptible to erosion and landslides (Shariffuddin and Udin, 2020). On the other hand, intensive agricultural activities are the main form of land use in this region, which has the potential to accelerate soil degradation if not balanced with the application of appropriate conservation techniques. A previous study conducted by Arsy (2008) reported that the Juwet sub-watershed has the highest erosion rate in the Oyo watershed, reaching 15.2 mm per year. Furthermore, research by Cahyadi et al. (2011) complemented these findings, estimating dissolved sediment loads of 102,079.5 tons per year and soil organic matter loss of 253.45 tons per year. These data indicate that the Juwet sub-watershed faces high erosion pressure, which has the potential to impact land quality decline, agricultural productivity decline, and increased risk of landslides and water quality degradation.

In accordance with national policy on watershed management as stipulated in Indonesia Government Regulation No. 37 of 2012, erosion control is one of the main components in maintaining the sustainability of watershed ecological functions. The selection of watershed management strategies needs to consider the achievement of land conservation targets based on actual problems in the field. Quantitative evaluation of soil erosion that focuses on identifying the contributing factors has been carried out by several researchers. Given that USLE is a simple mathematical model, sensitivity analysis can be performed through a simple approach such as OAT (one-at-a-time). This method can determine the percentage contribution of the most dominant factor as a conservation guideline. However, this method does not consider the synergistic effects of multiple factors on soil erosion. As is known, soil erosion occurs due to a combination of various factors, and this method is still insufficient to explain the complex multi-factor process of soil erosion (Ge et al., 2023). Nevertheless, the results of identifying dominant factors through OAT can serve as a basis for further research exploring interactions between factors using global sensitivity methods or machine learning-based approaches. Therefore, the scheme for determining conservation techniques is based on erosion determinants identified through this analysis (Fahmuddin and Widianto, 2004).

Against this background, this study aims to analyze erosion potential using the USLE modeling approach and analyze the sensitivity of USLE factors to facilitate spatially conservation planning in the Juwet sub-watershed. This objective can be achieved through: (1) mapping erosion factors including rainfall erosivity, soil erodibility, topography, land cover, and conservation practices, (2) analyzing model sensitivity to determine the dominant factors affecting erosion rates at the

watershed scale, and (3) designing conservation guidelines based on erosion determinants. Accordingly, this study aims to estimate soil erosion potential and to analyze the sensitivity of USLE parameters in the Juwet sub-watershed. The results are expected to clarify the relative contribution of major erosion-driving factors, which may support sensitivity-based erosion assessment and conservation prioritization in tropical hilly watersheds.

METHODOLOGY

Erosion potential analysis was conducted using the USLE model developed by Wischmeier and Smith (1978). This method is widely recognized for its usefulness when data availability is limited. This model estimates soil loss by integrating five key parameters shown in Figure 1. These five factors include rainfall erosivity (R), soil erodibility (K), slope length and steepness (LS), land cover and crop management (C), and soil conservation practices (P), according to Equation 1. Spatial analysis in this study used ArcMap to process the erosion data from USLE and generate a spatial distribution map of erosion risk. Sensitivity analysis was then performed using the one-at-a-time method to determine the most dominant factors contributing to erosion. Conservation guidance can be provided based on this sensitivity analysis for targeted management.

$$A = R \times K \times LS \times C \times P \qquad (1)$$

where: A – erosion potential (tons/year); R – rainfall erosivity factor (MJ mm ha^{-1} hour^{-1} year^{-1}); K – soil erodibility factor (tons ha hour MJ^{-1} mm^{-1}); LS – slope length and gradient factors (dimensionless); and CP – land cover and conservation factor (dimensionless).

Study area

The Juwet Sub-Watershed is part of the Oyo Watershed located in Gunungkidul Regency, Yogyakarta. The Juwet Sub-Watershed is located north of the Baturagung Hill area. It covers an area of approximately 32.8 km² and includes three main geomorphological zones based on topographical characteristics (Figure 2). The upper zone is located on the upper slopes of the ancient Nglanggeran volcano, the middle zone is located in the valley between structural ridges, and the lower zone occupies an alluvial plain with relatively gentle slopes. Topographically, the Juwet sub-watershed is located at an altitude of 118–807

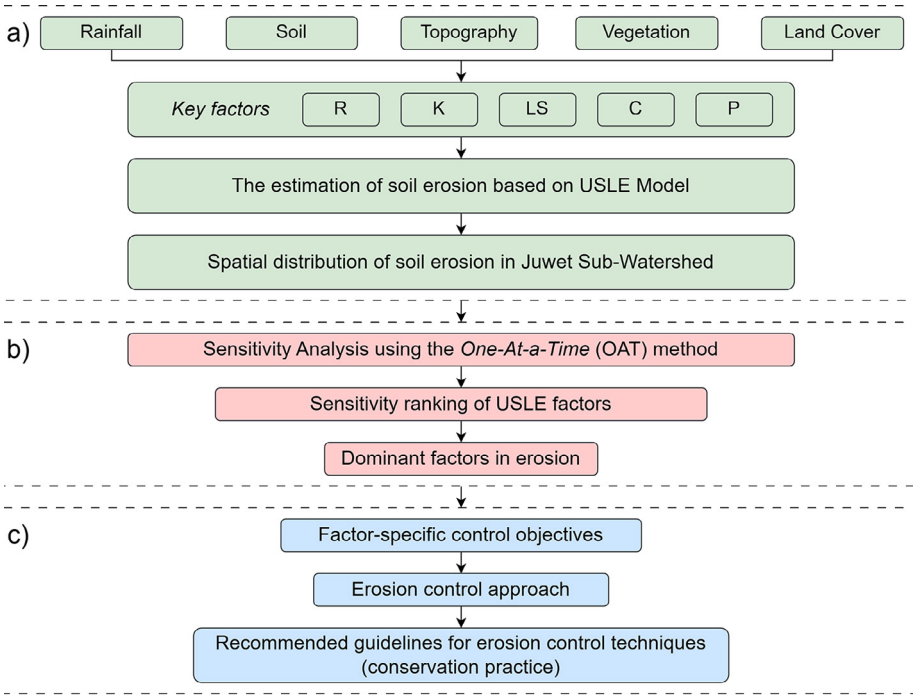

Figure 1. Research framework for soil erosion assessment and conservation planning: (a) erosion modeling using USLE, (b) sensitivity analysis using the OAT method, (c) soil conservation guidelines based on dominant factors

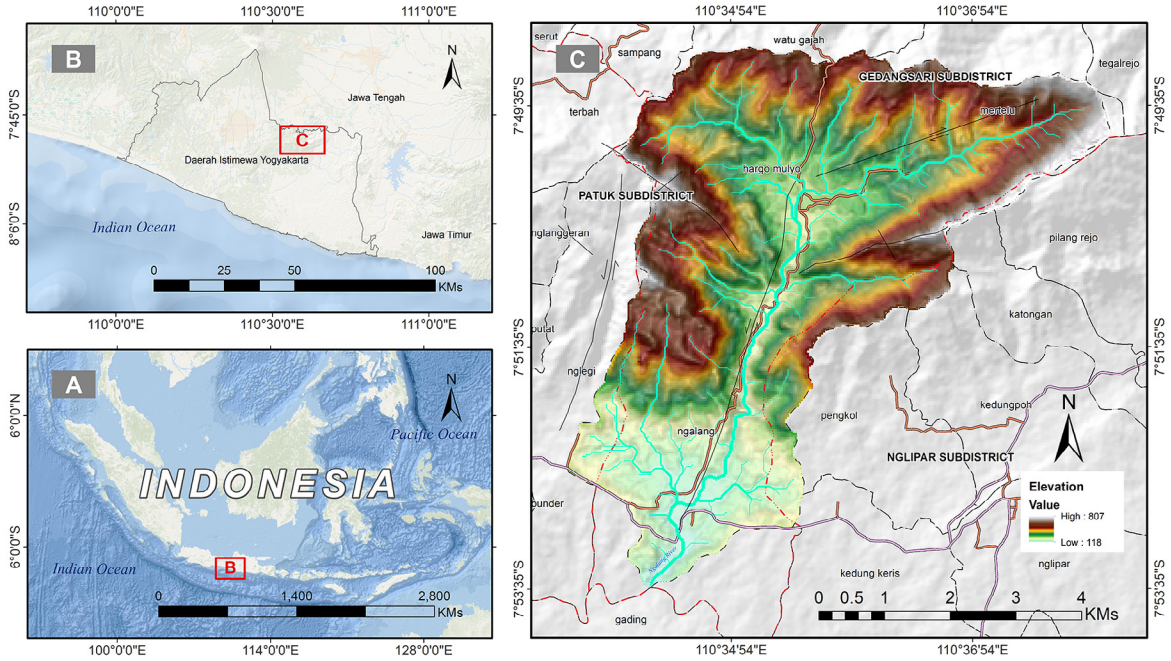

Figure 2. (A) Location of the study area in Indonesia; (B) location of the Juwet sub-watershed in the Special Region of Yogyakarta; (C) a detailed topographic map of the Juwet Sub-Watershed shows the distribution of elevation, river networks, and administrative boundaries covering three sub-districts: Gedangsari, Patuk, and Nglipar

meters above sea level (masl) with mountainous and structural-denudational hills, making it prone to erosion and mass land movement.

Geologically, this area consists of relatively impermeable volcanic and ancient marine sedimentary rocks, which affect soil infiltration capacity. Ongoing tectonic activity in this area can accelerate the rate of erosion, as the Juwet sub-watershed is located in a fault lithology contact zone (Saenkang et al., 2024). The combination of unstable lithological conditions, steep slopes, and high rainfall intensity creates conditions that are highly conducive to surface erosion.

The climate in this region is classified as a tropical monsoon climate, with the rainy season lasting from September to February. Annual rainfall is relatively high, but low soil absorption capacity causes most of the rainwater to become surface runoff. These conditions have the potential to cause flooding during the rainy season. Conversely, during the dry season, this region often experiences drought, characterized by a decrease in river flow to zero.

Morphologically, the Juwet sub-watershed area is dominated by hills with steep to very steep slopes, which occupy about 48.7% of the total area. Meanwhile, areas with flat to gentle topography have limited distribution, occupying about 1.6% and 9.1% of the total area, respectively. The central part of the sub-watershed forms a deep river valley with steep slopes, while the downstream part is dominated by relatively flat alluvial plains associated with the Oyo River. The dominance of steep topography is one of the main factors that increases the potential for erosion and highlights the urgency of implementing soil conservation measures in this area.

From a socio-economic perspective, the livelihood structure of communities around the Juwet sub-watershed is dominated by the agricultural sector, with more than half of the population depending on agricultural activities for their livelihoods. Intensive land use, especially on steep slopes, has increased the risk of erosion and accelerated soil fertility degradation, particularly in areas with low vegetation cover. These conditions demonstrate the close relationship between biophysical and social aspects of land management, making the implementation of community-based conservation practices key to maintaining ecosystem sustainability in the Juwet sub-watershed.

Data and sources

This study uses a combination of primary and secondary data. Primary data was obtained

through soil sampling in the field using a pedogeomorphological approach, specifically based on the geomorphological classification of landforms (Christanto et al., 2019). It is important to determine the landform first as a basis for determining the location of soil sampling. A landform map was created by combining geological and slope maps. Geological maps were sourced from the Ministry of Energy and Mineral Resources with a scale of 1:50,000 and were used to identify rock formations and lithological characteristics. In addition, a digital topographic map with a scale of 1:25,000 from the Geospatial Information Agency was used as a reference for administrative boundaries, river networks, and thematic map creation. The mapping resulted in 20 landform morphological units. One of these landform units was a outcrop without soil, so its value was 0, bringing the total number of samples to 19 units. Soil data collection was carried out by first determining the sampling points. The method used to determine the sampling points was purposive sampling. The location of soil sampling was determined by selecting one point in each landform classification. The determination of soil sampling locations was prioritized on undisturbed land, i.e., land that was considered to still have native soil. These locations were in forests, mixed gardens, and shrubbery. In addition, the determination of soil sampling locations was also based on considerations of location accessibility. The coordinates of each sample point were recorded using the Avenza Maps 5.5 application.

Field observations and soil sample observations were conducted in the field. Observations were made by observing the soil horizon, texture, root depth, and land use around the sampling site. Soil samples were taken by digging mini pits (25–30 cm deep) from the soil surface. The soil surface needed to be cleared of vegetation covering it. Soil samples were taken in disturbed and undisturbed conditions. Undisturbed soil samples were taken using a permeability ring, while disturbed soil samples were taken using a soil scoop. Approximately 1 kg of composite soil was collected per point. Soil samples were then tested in the laboratory to determine soil physical properties, including texture, structure, organic matter, and permeability, which formed the basis for determining the erodibility factor (K).

This approach assumes that soil formation differs under slope or flat conditions (Bao et al., 2025; Ewunetu et al., 2025). This approach was chosen because landform has low temporal variation, making it a potentially stable separation boundary (Keshavarzi et al., 2019). The relationship between landform and soil characteristics is very strong (Reddy et al., 2003), making landform the best indicator (Park and Burt, 2002) (Figure 3).

Secondary data includes various thematic maps and hydrometeorological data. Topographic data were obtained from the Shuttle Radar Topography Mission (SRTM) 1 Arc-Second Global dataset with 30-meter spatial resolution, which was downloaded from the United States Geological Survey (USGS) EarthExplorer platform (https://earthexplorer.usgs.gov/). Figure 4 illustrates the selection interface and spatial coverage of downloaded tiles compared to Juwet Sub-Watershed AOI (red polygon) confirms comprehensive coverage and no data gaps. The SRTM data acquisition process was methodical, including AOI delineation, dataset selection (SRTM), tile identification, and download in GeoTIFF format. Detailed processing steps are provided in Supplementary Material S2.

DEM acquisition was conducted through the USGS EarthExplorer platform following user authentication. The study area was defined by entering Gedangsari District as the geographic reference and manually defining an area of interest (AOI) polygon using sequential point marking. Each marked location generated geographic coordinates, which together created a closed polygon that defined the Juwet Sub-Watershed's extent.

The SRTM 1 Arc-Second Global dataset was chosen from the Digital Elevation catalog, with search results restricted to ensure comprehensive AOI coverage. Following metadata verification for spatial resolution (30 meters) and acquisition settings, the DEM tile (Entity ID: SRTM-1S08E110V3) was downloaded in GeoTIFF format to retain geographical referencing. Before processing, the file's integrity was verified.

The GeoTIFF file was imported into ArcMap 10.8 and reprojected using the WGS 1984 coordinate system. Following validation of spatial alignment with the watershed boundary shapefile, the DEM was clipped to the study area extent with the Extract by Mask tool, resulting in a spatially limited elevation dataset for subsequent terrain analysis. The Slope tool was then used to perform slope analysis, and the resulting slope raster was classed into six classes based on classification standards established by the Indonesian Ministry of Forestry. This classified slope map served as the

Figure 3. Field documentation and soil sample management: (a) mini pit preparation, (b) undisturbed soil samples were collected using a bulk density (BV) ring sampler, (c) disturbed soil sample collection and labeling, (d) air-dried soil samples prepared for laboratory testing, (e) soil sampling point locations displayed in Avenza Maps application, (f) undisturbed soil samples collected using bulk density rings, (g) field site conditions

foundation for assessing LS factors and evaluating erosion susceptibility inside the USLE modeling framework. Figure 4 and 5 illustrates the DEM acquisition and processing procedure in detail, including AOI delineation, dataset selection, preprocessing, and slope classification.

High-resolution aerial imagery was obtained from Bing Maps through SAS Planet software for land cover analysis. The imagery was acquired in September 2024, coinciding with the early rainy season when cloud cover was minimal, to ensure optimal image quality. The

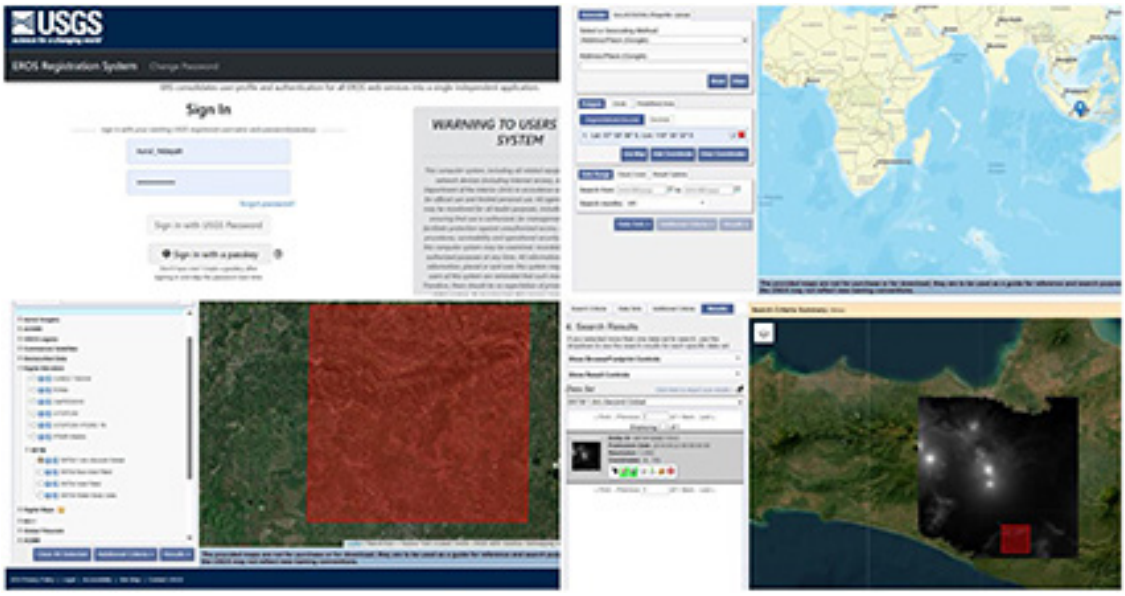

Figure 4. Step-by-step workflow of DEM acquisition using the USGS EarthExplorer platform: (a) access and login to EarthExplorer; (b) manual delineation of the Area of Interest (AOI); (c) selection of the SRTM 1 Arc-Second Global DEM (30 m resolution); (d) verification and selection of DEM tiles fully covering the study area

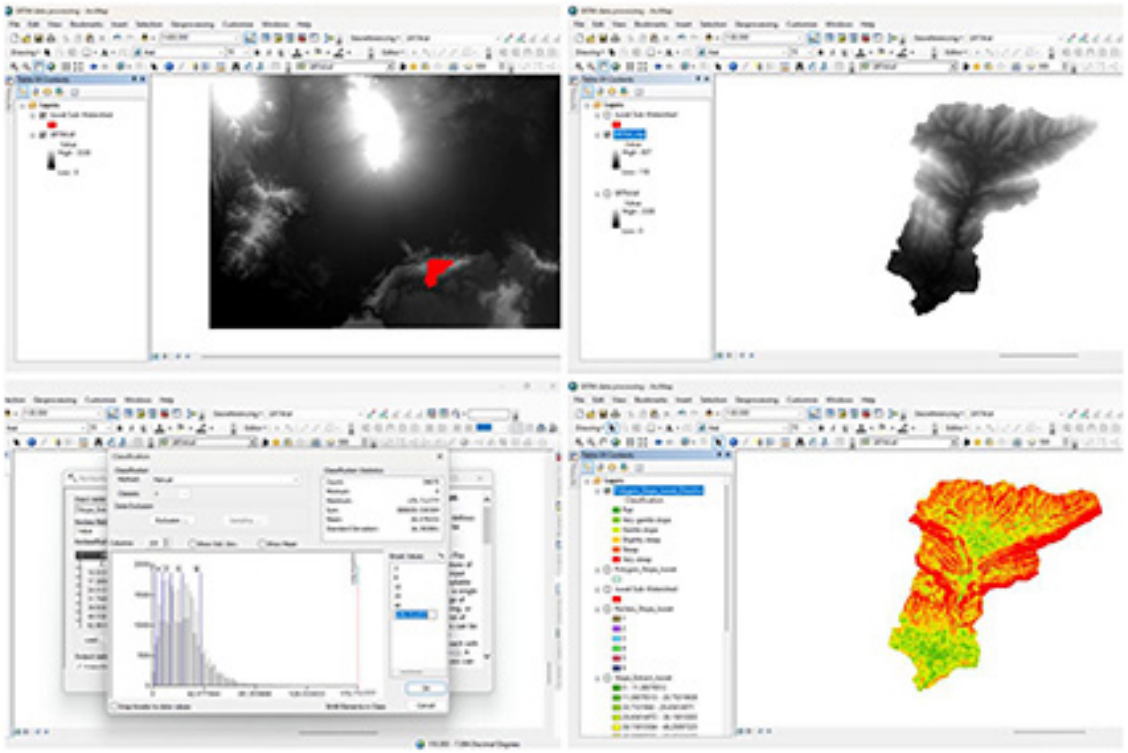

Figure 5. Step-by-step DEM processing for LS factor derivation: (e) DEM import and visualization in ArcMap 10.8; (f) clipping of the DEM to the Juwet sub-watershed boundary; (g) slope classification based on national standards; and (h) final slope class map used as input for LS factor estimation

downloaded imagery had a spatial resolution of 1.5 meters per pixel and covered the entire Juwet sub-watershed extent. This imagery served as the primary data source for visual interpretation and digitization of land cover types required for determining the cover management factor (C) in the USLE model. Land cover classification followed the Indonesian National Standard

(SNI 7645-1:2014) for land cover classification system.Ten years of rainfall data (2014–2023) from two rain stations (Kedungkeris and Beji Ngawen) were obtained from the Serayu Opak River Basir Basin Management Agency (BBWS) to calculate the rainfall erosivity factor (R) (Table 1).

Rain erosivity factor

The rainfall erosivity factor (R) describes the ability of rainfall to cause erosion through the kinetic energy it generates. Conceptually, the erosivity value is determined by a combination of rainfall kinetic energy and maximum rainfall intensity over 30 minutes (Benzougagh et al., 2022). This energy plays a role in releasing soil particles from their aggregates, thereby accelerating the process of soil release and transport (Lal, 1990). In practice, direct calculation of the R factor is often limited by the scarcity of rainfall intensity data at most observation stations. Therefore, a number of studies have developed empirical approaches based on monthly or annual rainfall data to estimate the R value (Ferro et al., 1991; Renard and Freimund, 1994).

The R factor was calculated using the conventional method proposed by Bols (1978) based on the average monthly rainfall function, the number of rainy days, and the maximum rainfall in a month (Equation 2). Rainfall data were obtained from the Kedungkeris and Beji Ngawen stations for the period 2014–2023. The data were processed into regional rainfall values to describe the distribution of rainfall in the Juwet Sub-Watershed area using GIS analysis with ArcGIS (Ulumia et al., 2025). This formula is recommended by the Indonesian Kementerian Kehutanan (2009) as a method suitable for the wet tropical climate conditions on the island of Java, as it is able to provide a fairly representative estimate of actual erosion potential.

$$R = \frac{6.199 \text{ x } P^{1.211} \times MaxP^{0.526}}{D^{0.474}} \quad (2)$$

where: R – monthly rainfall erosivity factor (MJ mm ha^{-1} h^{-1} year^{-1}); P average monthly rainfall (cm); D – number of rainy days in a month (without units); $MaxP$ – maximum rainfall in one month (cm).

Official data was acquired from the BBWS Serayu Opak web platform (https://sda.pu.go.id/balai/bbwsserayuopak/). The data was provided in tabulated format (.xlsx) and included daily and monthly rainfall quantities (mm), monthly totals, and maximum daily rainfall each month. Both stations provided continuous data coverage over a 10-year period (2014–2023). The 10-year period (2014–2023) was selected for three primary reasons: (1) The length is long enough to capture inter-annual rainfall variability and exceptional occurrences, resulting in accurate erosivity estimates (Renard and Freimund, 1994), (2) The data is up to date and relevant to the watershed's present climate and land use patterns, (3) Indonesian soil scientists recommend a minimum of 5–10 years for reliable erosivity estimate (Arsyad, 2010; Kehutanan, 2009).

Soil erodibility factor

Soil erodibility factor (K) is a function of several physical characteristics of soil, namely the percentage of silt and sand, organic matter content, soil texture, soil structure, and water infiltration capacity (Farhan and Nawaiseh, 2015). This parameter describes the strength of soil against the destructive power of rainwater kinetic energy and surface runoff, and reflects the average soil loss per unit of rainfall erosivity index (Parveen et al., 2012). The K value ranges from 0 to 1, indicating variations in soil sensitivity. A value close to 0 indicates high resistance to erosion, while a value

Table 1. Data and data sources

No.	Data	Data source
1	Rainfall data at Kedungkeris and Beji Ngawen Stations	Serayu Opak River Basir Basin Management Agency
2	Soil structure, permeability, organic C content percentage, and soil particle size fraction percentage at Juwet Sub-Watershed	Field survey and laboratory-tested
3	Shuttle Radar Topography Mission	United States Geological Survey (USGS)
4	Land use data	Bing aerial imagery and field-survey
5	Conservation practices	Bing aerial imagery and field-survey

close to 1 indicates low resistance (Cheikha et al., 2021). The soil erodibility value (K) is calculated using an equation developed by Yang et al. (2023) which is a modification of the Wischmeier and Smith (1978) formula with a conversion factor metric units (tons/ha) shown in equations 3 and 4. The erodibility value is calculated using the soil structure function, permeability, percentage of organic carbon content, and percentage of soil particle size fraction.

$$K = \frac{1.292\,[2.1\,M^{1.14}(10^{-4})(12-a) + +3.25(b-2) + 2.5(c-3)}{100} \quad (3)$$

$$M = \begin{pmatrix} percentage\ of\ very\ fine \\ sand\ and\ silt \end{pmatrix} \times \times (100\% - percentage\ of\ clay) \quad (4)$$

where: K – erodibility factor (tons ha hour MJ^{-1} mm^{-1}); M – percentage of very fine sand and dust x (100% – percentage of clay); a – percentage of organic matter (%); b – soil structure codes used in soil classification (see Table 2); c – soil profile permeability code (see Table 3).

All input parameters (M, a, b, and c) were determined through laboratory examination of 19 soil samples taken across the Juwet sub-watershed. Laboratory studies were performed at two ISO/IEC17025:2017 recognized facilities: Balai Penerapan Standar Instrumen Pertanian (BPSIP) Yogyakarta and Laboratorium Lapitaya Jasa Uji Lingkungan dan Pelatihan Lingkungan. Official certificates are CE.1/06.25/206 and 207/SPA/LTY/VII/2025. Soil texture with three fractions (sand, silt, and clay) reflecting the M parameter was obtained using the Hydrometer method as described in SNI 13-4691-1998. The organic carbon content (parameter a) was determined using the Walkley and Black method and laboratory code IK.5.4.d. The soil structure classification (parameter b) was derived using Balittan's (2023) classification, adapted from the USDA Soil Survey Manual. The soil permeability (parameter c) was measured using the De Boodt method.

Table 2. Soil structure code

No.	Soil structure class (Diameter size)	Code (b)
1	Granules are very fine (< 1 mm)	1
2	Fine granules (1–2 mm)	2
3	Granules are medium to coarse (2–10 mm)	3
4	Block-shaped, blocky, flat, solid	4

Slope length and steepness factor

The slope length and steepness factor (LS) reflects the influence of topography on erosion potential. This factor is a combination of two main components, namely slope length (L) and slope steepness (S), which together affect the amount of surface flow energy and its ability to transport soil particles (Jemai et al., 2021). In general, the longer the slope, the greater the volume of surface runoff produced, thereby increasing soil loss (Ganasri and Ramesh, 2016; Luvai et al., 2022). However, an increase in slope has been shown to have a more significant impact on accelerating erosion than an increase in slope length (Koirala et al., 2019).

The topographic factor was calculated using a digital elevation model (DEM) derived from SRTM. SRTM DEM data with a 30 meter spatial resolution were obtained from the USGS EarthExplorer platform (https://earthexplorer.usgs.gov/). The study area was defined by manually drawing an area of interest (AOI) polygon that encompassed the Juwet Sub-Watershed in Gedangsari District. The DEM was downloaded in GeoTIFF format and then imported into ArcMap 10.8 with the coordinate system set to WGS 1984. The SRTM raster was trimmed to the sub-watershed boundary to keep the analysis within the research region. Slope study was carried out using Spatial Analyst's Slope tool, with calculations expressed as percent rise and elevation units in meters. Using the Reclassify tool, the generated slope raster was categorized into six groups in accordance with the categorization guidelines established by the Indonesian Ministry of Forestry in 2009. The classified raster was converted to vector format using Raster to Polygon, followed by the Dissolve tool to merge polygons of the same slope class. The finished map was shown with a green-to-red color gradient that represented gentle to steep slopes. The LS factor values were then assigned to each slope class based on the classification criteria presented in Table 4.

Land cover factor

The land cover factor (C) reflects the influence of land management activities, agricultural practices, and vegetation on the amount of soil

Table 3. Soil profile permeability code

No.	Soil structure class (diameter size)	Permeability rate (cm/hour)	Code (c)
1	Very slow	<0.5	6
2	Slow	0.5–2.0	5
3	Slow to moderate	2.0–6.3	4
4	Moderate	6.2–12.7	3
5	Moderate to quick	12.7–25.4	2
6	Quick	>25.4	1

loss due to erosion (Almagro et al., 2019; Saoud and Meddi, 2023). The crop management factor refers to the combined influence of vegetation, litter, soil surface conditions, and land management on the amount of soil lost due to erosion (Assaoui et al., 2023). The C factor value ranges from 0 to 1, where a value of 1.0 indicates open land without vegetation cover (Table 5). Spatial and temporal variations in land cover can be identified through the use of remote sensing data, which allows for more accurate estimates of the C value (Meliho et al., 2020). Various studies have developed approaches to calculate the C value using different methods (Durigon et al., 2014). In this study, the classification of the C value was determined based on the criteria proposed by Arsyad (2010), which was considered most appropriate for the biophysical conditions of the study area.

Land cover mapping was done using ArcGIS software and on-screen digitization of high-resolution Bing Aerial Map imagery. To accurately designate land cover borders, the visual interpretation method included a variety of picture interpretation elements such as tone or color, form, size, texture, shadow, location (site), pattern, association, and evidence convergence. The classification structure was based on the Indonesian National Standard (SNI 7645-1:2014), which ensures uniformity and standardization.

Table 4. The value of the LS factor

Slope class	Slope gradient (%)	Classification	LS value
I	0–3	Flat	0.1
II	3–8	Very gentle slope	0.5
III	8–15	Gentle slope	1.4
IV	15–25	Slightly steep	3.1
V	25–40	Steep	6.1
VI	> 40	Very steep	11.9

The digitization procedure produced 6 various land cover types across the Juwet Sub-Watershed, such as mixed garden, paddy field, shrubland, settlement, natural forest, and production forest. Each polygon was manually outlined and given a land cover type code in the attribute table. The classification was confirmed and modified using field surveys, with ground truthing done at representative sampling locations to ensure the accuracy of the interpreted land cover classes.

Factor for erosion prevention/conservation efforts

The erosion prevention (P) factor describes the effectiveness of soil conservation efforts in reducing the rate of erosion. This factor ranges from 0 to 1, where a lower value indicates that conservation practices are being implemented effectively. Meanwhile, a value of 1 indicates that no conservation efforts have been made. The P classification in this study was conducted through direct field observations and image interpretation. The P factor refers to the criteria formulated by Arsyad (2010) listed in Table 6. This classification is used in research because it was specifically designed for soil conditions and conservation practices in Indonesia, taking into account the interaction between slope gradient and type of conservation practice, and it has been validated in multiple watersheds in Java with similar topographic and land use characteristics.

P factor assessment was conducted using a two-stage hierarchical approach. First, land cover classification from the previous stage (C factor analysis) provided a basic spatial consisting of six land cover types: mixed gardens, rice fields, shrubland, settlements, natural forests, and production forests. Second, within each land cover polygon, the presence or absence of specific conservation practices is determined through a combination of field observations and image interpretation. High-resolution aerial images were analyzed simultaneously to identify visible conservation patterns, such as terraced systems (stepped patterns on hillsides), contour planting (curved lines following elevation), and strip planting (alternating bands of crops across slopes).

Sensitivity of the USLE

Soil erosion is influenced by various factors including rainfall erosivity, soil erodibility, slope

Table 5. The value of factor C

No.	Land use	C value
1	Settlement/open land/without vegetation	1.0
2	Paddy field	0.01
3	Natural forest	0.001–0.005
4	Production forest	0.20–0.50
5	Mixed garden	0.10–0.50
6	Shrubland	0.30

Note: This table presents the C values for the main land use categories found in the Juwet sub-watershed. The complete classification for various types of crops and farming systems refers to Arsyad (2010).

length and steepness, as well as crop management and conservation practices. Each factor contributes differently to the amount of erosion. To identify the most influential factors as a basis for prioritizing conservation interventions, a sensitivity analysis was performed on the USLE model.

The OAT sensitivity analysis method was applied to measure the individual contribution of each input factor to the erosion rate. This method is used to identify dominant parameters that serve as priorities for conservation actions within the context of watershed management. In the OAT approach, one factor is systematically changed while all other factors are kept at their baseline values, allowing for the direct attribution of output changes to the modified parameter.

The sensitivity index (SI) for each factor is calculated using the following Equation 5. First, we identified erosion rate E as the response variable, which is derived as $E = R \times K \times LS \times C \times P$, with each USLE parameter (R, K, LS, C, and P) acting as an independent variable. We calculated baseline values for each metric using geographic averages over the Juwet sub-watershed. We obtained the minimum and maximum values for each parameter from the spatial mapping findings. Second, we tested three scenarios for each parameter. The baseline scenario computed erosion based on average values for all parameters. E_0 is calculated by multiplying $R_0 \times K_0 \times LS_0 \times C_o \times P_0$. The minimum scenario calculated erosion with one parameter at its minimum value while others remained at baseline. For example, testing parameter R: E-min(R) = R_min $K_0 \times LS_0 \times C_o \times P_0$. We repeated the process for each parameter, returning to baseline circumstances in between tests. Third, we examined the data to determine the major factor. We determined dominance by examining which parameter generated the greatest change in erosion relative to its input change. We derived three metrics for each parameter: absolute erosion change ($\Delta E = E_{max} - E_{min}$), relative input change ($\Delta X/X_0 = (X_{max} - X_{min})/X_0$, and sensitivity index ($SI = ((\Delta E/E_0) / (\Delta E/E_0 / (\Delta X/X_0)) \times 100\%$). A higher SI value indicates greater sensitivity of the erosion model to specific factors, thus identifying priority areas for conservation intervention.

$$SI = \frac{|\frac{\Delta E}{E_0}|}{|\frac{\Delta X}{X_0}|} \times 100\% \quad (6)$$

where: *SI* – sensitivity index, represents the percentage change in erosion output per unit percentage change in the input parameter; ΔE – absolute change in soil loss from baseline (ton/ha/year); E_0 – baseline soil loss (ton/ha/year); ΔX – change in input parameter value; and X_0 – baseline value of input parameter.

Table 6. Value of factor P

No.	Forms of conservation	Code (c)
1	Bench terrace – good condition	0.04
2	Bench terrace – moderate condition	0.15
3	Bench terrace – poor condition	0.40
4	Traditional terrace	0.35
5	Contour ridges – good condition	0.15
6	Permanent grass strips – good condition, dense, and well-aligned	0.04
7	Permanent grass strips – poor condition	0.40
8	No conservation measures	1.00

Land conservation planning

Land conservation planning was created to integrate sensitivity analysis results into spatially explicit and conservation initiatives. Erosion in watersheds is caused by multiple interacting factors. While sensitivity analysis can identify the most influential factors, field implementation requires spatial delineation of these factors across the landscape. The goals of this conservation planning framework are to: (1) identify and demarcate priority zones based on the spatial distribution and combined severity of dominant erosion factors identified through sensitivity analysis; (2) assign specific conservation techniques to each zone based on dominant factor characteristics; and (3) develop an implementation framework prioritized by erosion severity and intervention urgency. This method ensures that conservation initiatives are systematically matched to site-specific erosion drivers, resulting in efficient resource allocation and maximum erosion control effectiveness.

To facilitate spatially explicit conservation planning, continuous erosion factor from USLE modeling were grouped into management-relevant groups. The reclassification focused on dominant characteristics revealed by sensitivity analysis, which are the major leverage points for erosion control actions. The erosion factor layers (R, K, LS, C, and P) derived from USLE modeling were reclassified into categories relevant to management. Factors identified as dominant through sensitivity analysis were then spatially stratified to capture the range of conditions across the watershed. Cross-tabulation of these stratified factors enables the identification of zones with different combinations of factor severity levels.

Each spatial zone is assigned a priority level based on the combined severity of the dominant erosion factors. The priority classification is validated by testing the correlation between the assigned priority levels and the actual erosion rates calculated from USLE modeling, using Spearman's rank correlation to assess the discriminatory power of the classification system. Conservation techniques are matched to each priority zone following the decision framework in Figure 5, which links dominant erosion factors to appropriate control measures. The selection of techniques considers: (a) specific factors requiring control based on sensitivity analysis, (b) local biophysical conditions (slope, soil type, land use), and (c) feasibility of implementation.

The determination of the type of conservation technique refers to the classification by Fahmuddin and Widianto (2004), which categorizes conservation methods based on the dominant factor causing erosion. This framework connects each USLE factor with specific conservation techniques as presented in Figure 5. Although each factor has a specific handling path, it is important to understand that the determinants of erosion are closely interconnected in the soil erosion process. The recommended conservation techniques are not limited to addressing only the dominant factors, but can include approaches that have a synergistic effect on other factors.

The implementation of conservation guidelines is carried out by identifying dominant factors based on the highest SI obtained from sensitivity analysis. Next, the conservation technique is selected based on the dominant factor using the decision matrix in Figure 6. The selection of techniques is contextually adapted, considering local biophysical and socioeconomic conditions to ensure the suitability and sustainability of implementation. This approach aligns with modern conservation principles that emphasize investment efficiency through targeted interventions (Srivastava et al., 2024). By identifying and targeting the drivers of erosion, the impact of erosion reduction can be maximized with limited resources.

RESULTS AND DISCUSSION

Rainfall erosivity factor

The analysis of rainfall erosivity factor (R) in the Juwet sub-watershed is based on annual temporal rainfall data from 2014–2023 obtained from the two nearest rain stations, namely Kedungkeris and Beji Ngawen. The spatial distribution of rainfall was calculated using the Thiessen Polygon method to determine the coverage area of each station based on monthly recorded data. Some parameters used in calculating rainfall erosivity include average monthly rainfall (cm), the number of rainy days in a month (unitless), and maximum rainfall in a month (cm). The rainfall erosivity factor at each station is calculated based on the average monthly erosivity value for the period 2014-2023.

The erosivity values obtained at each station are 1500.38 for Kedungkeris and 1232.4 for Beji Ngawen, with units of $MJ \cdot mm \cdot ha^{-1} \cdot h^{-1} \cdot year^{-1}$

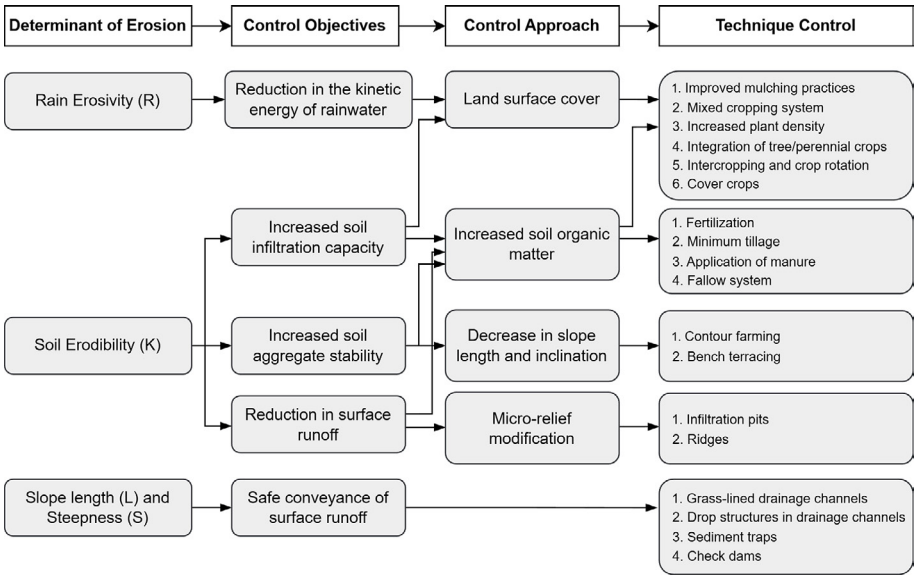

Figure 6. Framework for soil conservation guidelines based on erosion determinants, control objectives and approaches, and applicable control techniques (modified from Beets, 1990)

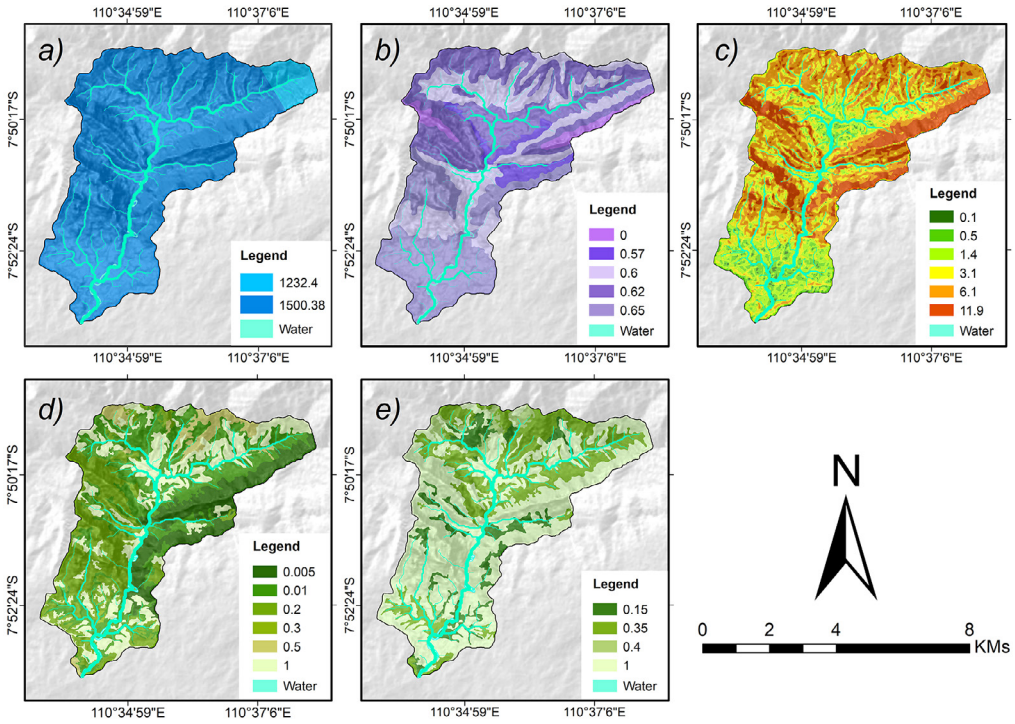

Figure 7. Spatial distribution of USLE factors in the Juwet sub-watershed: (a) rainfall erosivity factor (R) ranges from 1,232.4 to 1,500.38 MJ·mm·ha^{-1}·h^{-1}·year^{-1}; b) soil erodibility factor (K) shows higher values in the Nglanggeran and Sambipitu Formations with a range of 0.57–0.65 tons.ha.hour.MJ^{-1} mm^{-1}; (c) topographic factor (LS) with steep slopes (25–40%) is concentrated in the central and upstream zones; d) crop management factor (C) indicates the dominance of paddy fields (31.24%) and settlements (23.55%); (e) conservation practice factor shows limited implementation with values of 0.15–1.0, where most areas (>60%) have not implemented adequate conservation practices

(Table 7). The recorded rainfall erosivity value is 1487.585 MJ·mm·ha^{-1}·h^{-1}·year^{-1}, with a seasonal pattern showing peak erosivity in February–March and November–December, and a significant decrease during the dry period between May–September (Figure 7). This temporal variation aligns

with the monsoon rainfall patterns in southern Indonesia, where the rainy season is caused by the dominance of the west monsoon winds bringing moist air masses (Aldrian and Susanto, 2003). The undulating topographic conditions in the Juwet Sub-Watershed, which is part of the Baturagung Hills, also intensify rainfall through the process of orographic rain. As a result, this area has the potential to experience higher rates of erosion compared to the surrounding plains.

The erosivity value in the Juwet sub-watershed is comparable to that reported in several watersheds in Indonesia with similar monsoon climate characteristics. Zawiyah et al. (2024) reported an R value of 1,362.79 MJ·mm·ha^{-1}·h^{-1}·year^{-1} in Nagari Lawang, West Sumatra, which falls within the same range. Mechanically, increased rainfall intensity is directly proportional to the kinetic energy of raindrops, which accelerates soil aggregate breakdown and particle release to the surface (Mineo et al., 2019). This finding confirms that the wet months in the hilly region are a critical period for erosion risk. This aligns with research findings Wang et al. (2024) indicating that hilly areas have a greater potential for runoff and soil loss due to high rainfall intensity.

Soil erodibility factor

The soil erodibility factor indicates the soil's susceptibility to erosion and surface runoff. The K factor was derived from the geomorphological landform map of the Juwet sub-watershed and soil analysis. The physical data for estimating soil erodibility were obtained from collected soil samples covering the study area. These samples were analyzed to determine soil texture (sand, silt, and clay content), permeability, structure, and organic matter. The Juwet sub-watershed is located on structural landforms with diverse morphologies, inclusing crest, upper slopes, middle slopes, lower slopes, foothills, colluvial, and alluvial plains. In the concept of pedogeomorphology, each morphological unit represents a K value. Based on 19 soil samples analyzed in the laboratory, the K value ranged from 0.57 to 0.65, indicating a moderate to high level of erodibility according to the USDA classification. Table 8 and Figure 7 shows the distribution of K values in each landform morphology in the Juwet sub-watershed. Meanwhile, Figure 8 depicts the regional distribution of soil samples.

The spatial distribution of K values shows a pattern related to geological formations and landforms. The lowest value (0.57) was found in the Lower Kebobutak Formation Plain and the Lower Nglanggeran Formation Slope, while the highest value (0.65) was found in the Nglanggeran and Sambipitu Formations. High K values are generally found in soils with high clay content. These conditions are evident on the middle slope of the Nglanggeran Formation and the Sambipitu Allvial Plain. Soil with high clay content is highly susceptible to erosion, especially when vegetation cover is minimal. Although the particles are difficult to dislodge, clay soil has low permeability, resulting in high surface runoff and susceptibility to erosion by rainwater. In contrast, sand soils exhibit more stable aggregates and lower K values.

Soil structure can affect aggregate stability and water infiltration, while soil texture affects the soil's ability to retain and drain water. The coarser the soil texture, the lower the soil's ability to retain water. Based on the data obtain, granular structure produce low K values, while blocky or massive structures increase susceptibility to erosion due to poor aggregation and dense pores. Samples from several locations show block structures with high K values. Soil permeability in the Juwet sub-watershed varies between 0–7.63 cm/hour, with a negative correlation to K values. Soils with very slow permeability (<1 cm/hour), such as in the Sambipitu and Oyo Formations, have high K values (0.65), while soils with moderate permeability show lower K values. Low infiltration increases surface runoff,

Table 7. Rainfall erosivity in the Juwet sub-watershed based on rainfall weighting

Rain station	Rainfall erosivity (R)	Area (A) (km^2)	RxA
Kedungkeris	1,500.38	31.31	46,976.9
Beji Ngawen	1,232.4	1.57	1,934.9
Total		32.88	48,911.8
Rainfall erosivity (R)			1,487.585

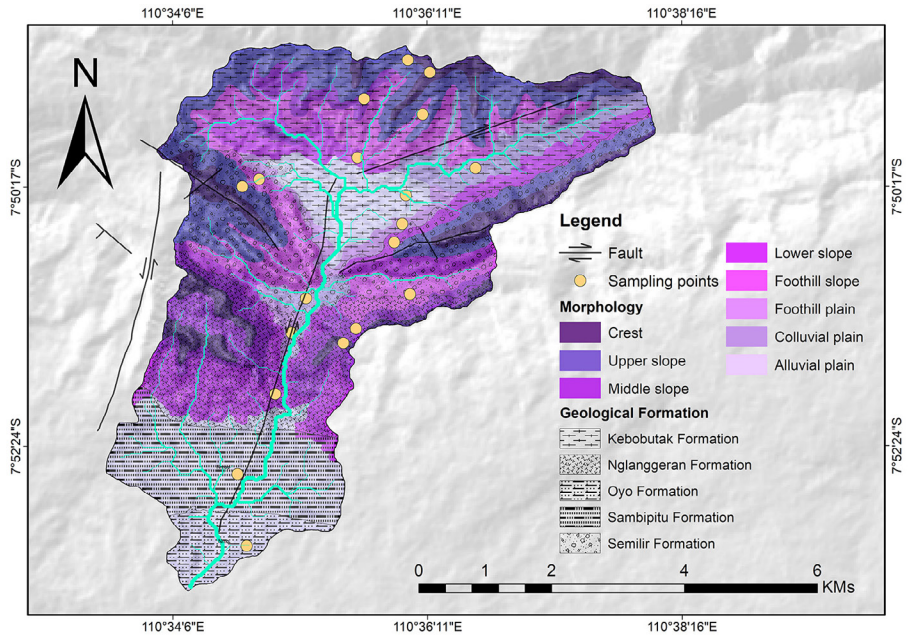

Figure 8. Map of landforms and soil sampling points in the Juwet sub-watershed

which accelerates erosion (Hacisalihoğlu et al., 2019; Zhang and Yu, 2023).

Soil organic matter in this region is classified as low to moderate (0.34–2.23%). Although it plays an important role in improving soil structure and aggregation (Satriagasa and Suryatmojo, 2020), no consistent correlation was found between organic matter content and K values. This indicates that the influence of soil texture and structure is more dominant on the level of erodibility in the Juwet sub-watershed.

Slope length and steepness factor

Slope information for the Juwet Sub-Watershed was obtained from processing SRTM data. The LS value classification refers to the Regulation of the Minister of Forestry of the Republic of Indonesia (2009) concerning Procedures for Preparing Technical Plans for Forest and Land Rehabilitation in Watersheds (RTkRHL-DAS). The analysis results show that the Juwet Sub-Watershed area is dominated by a slope class of 25–40%, which indicates a hilly topography with fairly steep morphology. This condition indicates a high potential for erosion, as steeper slopes accelerate sediment transport and increase surface flow strength (Zhang and Yu, 2023).

Table 9 presents a detailed classification of slope categories and corresponding LS values in the Juwet sub-watershed. The distribution of slope gradients is shown in Figure 7, which illustrates the spatial variation of LS with a color gradient from green to red. The dominant orange to red colors in the central and northern parts (upstream areas, especially Gedangsari District) indicate areas with high LS indices (>3.1), which indicate steep to very steep slopes. Increased slope inclination in these areas accelerates surface runoff and sediment transport, thereby increasing the risk of erosion.

Land cover factor

The watershed was divided into six land use types based on manual interpretation of satellite imagery data and extensive field studies. The allocated crop cover factor values were used to construct a C-factor map for the overlay analysis. Based on the land use classification**,** land use in the Juwet Sub-Watershed is dominated by rice fields covering an area of 1,027.37 ha (31.24%), followed by production forests (24.2%), settlements (23.55%), protected forests (14.90%), mixed gardens (5.27%), and shrubs (0.2%). The spatial pattern of land use shows zoning based on topography and accessibility: flat and easily accessible areas are dominated by settlements and rice fields, while steep hilly areas are covered by forests and mixed gardens. The presence of the Ngalang River also influences the distribution

Table 8. Soil erodibility (K) in the Juwet sub-watershed

Landform Morphology	Texture (%)			M	a	b	c	K
	Sand	Silt	Clay					
Crest of Kebobutak Formation	30	40	30	4900	0.35	4	4	0.60
Upper slope of Kebobutak Formation	26	44	30	4900	2	4	5	0.62
Middle slope of Kebobutak Formation	35	40	25	5625	0.34	3	5	0.62
Foothill plain of Kebobutak Formation	30	43	27	5329	1.17	3	4	0.60
Lower slope of Kebobutak Formation	34	38	28	5184	0.51	2	4	0.60
Colluvial plain of Kebobutak Formation	30	32	38	3844	1.25	4	5	0.62
Alluvial plain of Kebobutak Formation	15	45	40	3600	2.23	4	5	0.62
Foothill plain of Semilir Formation	30	33	37	3969	0.71	3	5	0.62
Upper slope of Semilir Formation	61	22	17	6889	0.89	4	5	0.62
Foothill plain of Kebobutak Formation	39	35	26	5476	0.47	2	3	0.57
Foothill plain of Nglanggeran Formation	25	35	40	3600	1.33	4	4	0.60
Lower slope of Semilir Formation	27	35	38	3844	0.59	4	3	0.57
Colluvial plain of Semilir Formation	21	33	46	2916	0.76	4	4	0.60
Lower slope of Semilir Formation	26	46	28	5184	0.76	4	4	0.60
Middle slope of Nglanggeran Formation	15	33	52	2304	0.91	4	6	0.65
Crest of Nglanggeran Formation	27	30	43	3249	1.4	4	6	0.65
Lower slope of Nglanggeran Formation	46	30	24	5776	0.43	3	4	0.60
Alluvial plain of Sambipitu formation	6	37	57	1849	1.37	4	6	0.65
Alluvial plain of Oyo formation	20	42	38	3844	1.78	4	6	0.65

pattern of rice fields, especially irrigated rice fields in the central plains.

Each type of land cover has a different level of soil protection against erosion. Protected forests have the lowest C value (0.005) due to high vegetation density and litter layers that can absorb the kinetic energy of rain and slow down water flow. These biophysical conditions help reduce direct contact between water and the surface. In contrast, production forests and mixed plantations show higher C values due to anthropogenic interventions such as logging or soil cultivation, which reduce canopy density and increase erosion potential (Hacisalihoğlu et al., 2019). Residential areas and rainfed rice fields also contribute to increased surface runoff due to limited water absorption, especially in densely populated lowlands.

The use of land for paddy fields also has a relatively low C value (0.01) because the soil is generally left flooded, making it resistant to erosion and surface runoff. Meanwhile, mixed gardens have a moderate C value. Mixed gardens in the study area are dominated by tree species such as banana, sengon, teak, cassava, and corn. These plants protect the soil from erosion, but canopy cover in mixed gardens decreases during the dry season. Settlements have the highest C value among other types of land use. The high C value in settlements is due to low or no vegetation. This condition has the potential to increase surface runoff.

Table 9. LS classification in the Juwet sub-watershed

Slope (%)	Slope classification	Length and steepness (LS)	Area (ha)	Percentage (%)
0–3	I	0.1	51.32	1.56
3–8	II	0.5	299.4	9.10
8–15	III	1.4	565.6	17.20
15–25	IV	3.1	769.73	23.40
25–40	V	6.1	1,057.37	32.15
>40	VI	11.9	545.39	16.58

Factor for erosion prevention/conservation efforts

The determination of the P factor in the Juwet sub-watershed was carried out through field observations and interpretation of Bing aerial imagery and Google Earth images. Soil conservation plays an important role in controlling the erosion process. Soil conservation is described as a practice that can significantly prevent erosion (Blanco and Lal, 2008). Based on the analysis results, land with natural uses such as natural forests, production forests, mixed gardens, and shrubs generally does not yet have adequate conservation. Meanwhile, rice fields, which dominate the Juwet sub-watershed, have mostly implemented conservation techniques in the form of terrace systems.

The use of paddy fields shows the application of various soil conservation techniques. Of the total 1,028.78 ha of rice fields, 97.8% have implemented conservation techniques, while only 0.64% (20.98 ha) have no conservation efforts. The most dominant conservation technique is traditional terraces covering an area of 596.61 ha (18.14%), followed by medium terraces covering an area of 312.69 ha (9.51%). Paddy field management on steep and very steep land has used a gulud terrace system that combines elephant grass on the edge of the terrace. This grass is used by the community as livestock feed. However, this conservation technique is considered ineffective when applied to land with steep and very steep slopes. According to Satriagasa and Suryatmojo (2020), grass cover on paddy fields with a gulud terrace system can only reduce maximum erosion accumulation on land with a slope of 15–25%.

The lowest value of P factor of 0.15 represents conservation in the form of well-managed medium terraces and contour ridges. Almost all paddy fields in the Juwet sub-watershed have conservation features in the form of bench terraces and traditional terraces. Functionally, these terraces help reduce the amount and speed of surface runoff, allowing the soil to absorb or retain more water. Therefore, the soil structure becomes stable because the destructive force on the soil is reduced (Martins et al., 2025).

Paddy fields with terraces and traditional terraces are also found on land with moderately steep to steep topography. Meanwhile, rice fields without conservation measures are located in areas that tend to be flat on alluvial plains on the southern side of the sub-watershed. In flat areas, terraces are not necessary because surface runoff is minimal. The construction of bench terraces is adjusted according to contour lines, which are useful in reducing the speed of surface runoff, and the vegetation on these lines is able to filter and trap sediment effectively (Kuok et al., 2013). Traditional terraces and bench terraces are considered more effective than poorly constructed bench terraces, as indicated by lower P values (0.35 and 0.15 compared to 0.4). This difference indicates the importance of the quality of terrace construction and maintenance in determining the effectiveness of soil conservation.

The multiplication of C and P values is directly proportional to erosion potential. A low CP index value indicates low erosion potential, and vice versa. This means that a low CP value indicates more effective land management and conservation efforts (Alves et al., 2022). Spatially, the spatial distribution of C and P values in the Juwet sub-watershed can be seen in Figure 7. The CP value for water bodies (rivers) is set to zero (0), assuming no erosion occurs in these places (Table 10).

Erosion potential in the Juwet sub-watershed

The estimation of soil erosion potential in the Juwet sub-watershed was conducted using the USLE model. This model integrates five factors comprising rainfall erosivity, soil erodibility,

slope length and steepness, cover management, and conservation practices to quantify the spatial distribution of erosion on an annual basis. Analysis and evaluation of these primary USLE parameters are essential for understanding erosion processes and enabling the development of spatially erosion susceptibility maps across the study area. Spatial overlay analysis of all five factors was performed using GIS-based polygon intersection, yielding a total annual erosion potential of 1,775,551.95 tons/year for the entire sub-watershed. The spatial distribution of erosion rates was classified into five categories following the classification standards established by the Indonesian Ministry of Forestry (Kementerian Kehutanan, 2009) as presented in Table 11. Figure 9 illustrates the spatial distribution of erosion rate classes and their respective areal coverage within the Juwet sub-watershed.

According to the analysis results, erosion rates in the Juwet sub-watershed range from very moderate to very heavy. Figure 5 shows that the research area is dominated by the extremely heavy erosion rate class (≥480 tons/ha/year). The spatial distribution of erosion classes exhibits diverse patterns throughout the sub-watershed. The very heavy erosion class (≥480 tons/ha/year) accounts for 1,390.00 km² or 42.26% of the total area, mostly concentrated in settlement complexes and mixed plantation zones. The extremely light class comes in second with an area of 25.43%, while the middle class (60–180 tons/ha/year) has the smallest percentage, at only 3.16% of the entire area. The domination of the extremely heavy class highlights the importance of serious soil and water conservation initiatives in the area.

The estimated erosion results are compared to those of prior studies. According to Arsy (2008), the Juwet sub-watershed has the highest erosion rate in the Oyo watershed, reaching 15.2 mm per year, which equates to around 190–228 tons/ha/year (assuming a soil bulk density of 1.25–1.5 g/cm^3). Meanwhile, Cahyadi et al. (2011) estimated suspended sediment at 102,079.5 tons per year, revealing the true erosion rate in this area. This quantitative comparison gives a reference range for determining the validity of the USLE model's results.

The average erosion rate in the Juwet sub-watershed is 54.03 tons/ha/year, indicating severe land degradation that substantially exceeds Indonesia's soil erosion tolerance threshold of 12 to 25 tons/ha/year (Arsyad, 2010). Zawiyah et al. (2024) reported an average erosion rate of 3.32 tons/ha/year, which is approximately 16 times lower than in the Juwet sub-watershed. Although both regions have hilly terrain, Nagari Lawang's land use is dominated by woods and natural plants, providing better erosion protection. Meanwhile, agricultural land intensification in the Juwet sub-watershed occurs in the absence of proper conservation methods.

USLE sensitivity analysis

The analysis results show that the erosion rate in the Juwet sub-watershed is highly influenced by two main factors: slope length and steepness and land cover, as presented in Table 12. The LS factor is the most sensitive parameter with the highest

Table 10. CP in the Juwet sub-watershed

Land use	C	Conservation management	P	CP	Area (ha)	Percentage (%)
Waterbody	-	-	-	-	21.28	0.65
Natural forest	0.005	No conservation	1	0.005	489.99	14.90
Production forest	0.2	Traditional terraces	0.35	0.07	77.73	2.36
		No conservation	1	0.2	718.01	21.83
Mixed garden	0.5	Traditional terraces	0.35	0.175	161.49	4.91
		No conservation	1	0.5	11.69	0.36
Settlement	1	No conservation	1	1	774.63	23.55
Paddy field	0.01	Bench terrace, moderate	0.15	0.002	312.69	9.51
		Bench terrace, poor	0.4	0.004	90.71	2.76
		Traditional terraces	0.35	0.01	596.61	18.14
		No conservation	1	1	20.98	0.64
		Good contour ridges	0.15	0.002	6.38	0.19
Shrubland	0.3	Poor permanent strip cropping	0.4	0.12	6.65	0.20

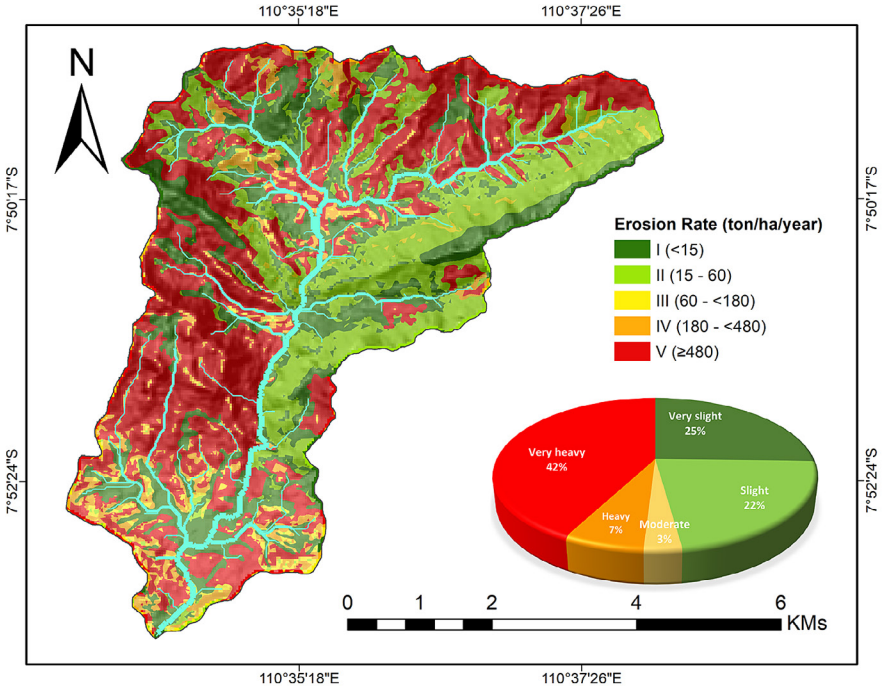

Figure 9. The spatial distribution of erosion rate classes in the Juwet sub-watershed shows that highly heavy erosion zones are mostly found in settlement complexes and mixed garden areas, whereas natural forest zones constantly have the lowest erosion rates. The area distribution of erosion level classes in the Juwet sub-watershed, according to the Ministry of Forestry classification (2009)

absolute change range, which is 3253.89 tons/ha/year. This indicates that topographic conditions play a significant role in determining the erosion potential at the study site. The steeper the slope, the higher the speed and energy of the surface runoff formed, thus increasing the potential for erosion. The range of values for the LS factor is relatively wide (0.1–11.9), indicating that differences in slope are the main cause of high erosion susceptibility in the Juwet sub-watershed.

The land cover factor is in second place with an absolute change range of 2543.98 tons/ha/year. The high sensitivity of the C factor indicates that vegetation conditions and land cover types play an important role in controlling erosion. The C value, which varies from 0.01 (for dense forests) to 1.0 (for open land/settlements), illustrates the extent to which vegetation can protect the soil from rainfall energy and surface runoff. This means that any change in vegetation type or density will impact the potential for erosion. Efforts to increase land cover, which can be achieved thru reforestation, agroforestry, or multi-layered cropping systems, are a strategic step to reduce erosion. This finding aligns with the statements of Feyereisen et al. (2007) and Arsyad (2010), who mentioned that the most sensitive factor to erosion is generally influenced by the land use itself.

The soil conservation factor is in third place with a change range of 1246.82 tons/ha/year. Although its influence is not as significant as LS and C, this factor is still important because it is related to mechanical conservation practices such as contour terraces and soil retaining walls. However, the effectiveness of P is highly dependent on slope conditions and the presence of vegetation. The rainfall erosivity factor shows a relatively small range of variation in value, with an absolute change of 191.78 tons/ha/year and a relative contribution of 0.20%, placing it in the fourth dominant category. This condition can be explained by the geographical characteristics of the Juwet sub-watershed, which is classified as a micro-watershed with a relatively small area. As a result, the spatial variability of rainfall within the study area is limited, leading to a spatially homogeneous distribution of rainfall erosivity.

Beside the small watershed area, the rainfall erosivity parameter with low sensitivity is also influenced by the data collection used in this study. Rainfall data was obtained through interpolation techniques from rainfall stations outside the study area (ungauged stations), as there were no rainfall

Table 11. Distribution of erosion susceptibility in the Juwet sub-watershed

Susceptibility level	Erosion rate (ton/ha/year)	Area (ha)	Pecentage (%)
Very low	<15	836.24	25.43
Low	15–60	735.45	22.36
Moderate	60–180	103.85	3.16
Severe	180–480	223.28	6.79
Very severe	>480	1390.00	42.26

observation stations located within the Juwet sub-watershed. Interpolation methods such as the Thiessen Polygon applied to data from external stations tend to produce relatively uniform erosivity values across the entire study area, especially when the distance between observation stations is quite far and the number of stations is limited. The ungauged condition of this station is a common challenge in hydrological research in Indonesia, particularly in small watersheds that lack adequate monitoring infrastructure. However, the interpolation approach from the nearest station remains an acceptable method in erosion modeling, provided that the interpolation results consider the limitations of representing the actual spatial variability of rainfall. The implication of the low sensitivity of this rainfall erosivity parameter is that in the context of erosion management in the Juwet sub-watershed, intervention efforts do not need to be directed toward the temporal and spatial variability of rainfall, but rather toward factors that can be managed directly, namely topography (through mechanical conservation techniques) and land cover (through vegetative conservation).

However, the USLE model also tends to underestimate high erosion values. This resulted in two distinct data populations in the calculation results, likely due to geographical variations and extreme environmental conditions in the study area. Similar conditions were also found by Zhang and Yu (2023) in their study in mountainous regions, where complex and heterogeneous topographic characteristics led to significant differences between model values and actual field conditions.

Overall, the results of this sensitivity analysis confirm that erosion control in the Juwet sub-watershed must be implemented through an integrated and tiered conservation strategy. Improving and maintaining land cover needs to be a top priority because this factor is the most easily controlled by humans and has the greatest impact on reducing erosion. Areas with high LS values should be designated as primary conservation zones receiving special attention through the application of mechanical conservation techniques (P factor) and increased protective vegetation. Thus, the combination of managing the dominant physical factors and optimizing human-controllable factors becomes the key to effective and sustainable erosion control in the Juwet sub-watershed.

Furthermore, the dominance of the LS (topographic) and C (land cover) factors in this study is not merely a local phenomenon, but also reflects the fundamental structure of the USLE model itself. Each factor (R, K, LS, C, and P) is multiplicative, and the scale of its influence depends heavily on the value of each input and its range of variability. Because factors LS and C often have a very large range of values and are physically highly variable, they tend to be the largest contributors to variance in erosion rates compared to other factors with more limited variability (such as K or R). For example, a systematic study by Panagos et al. (2015) showed that LS is one of the critical factors in determining soil loss due to the combination of slope length and steepness, which affects sediment transport (Gezici et al., 2025).

Additionally, other literature mentions that at both the land and sub-watershed scales, the LS and C factors frequently appear as dominant factors in sensitivity analyzes. For example, in a review of the USLE/RUSLE model factors, it is stated that the topographic factor and the cover-management factor are factors that significantly influence the overall efficiency of the model (Oliveira et al., 2013). The research findings in the Juwet Sub-Watershed, which show the significant contribution of LS and C, can be theoretically justified. The USLE model indeed prioritizes topographic and land cover conditions as key variables in erosion estimation, particularly in environments with clear differences in slope and vegetation, such as the study area. This reinforces the conclusion that erosion management interventions need to be more focused on these factors, as they are both the most sensitive and have the greatest impact on the model and on the reality in the field.

Land conservation planning

The sensitivity analysis results indicate that the LS and C factors are parameters that influence the rate of soil erosion in the study area. These two factors were selected as control factors for conservation measures. Based on the sensitivity

analysis results, a two-factor priority matrix was developed by overlaying the LS and C factor maps that had been reclassified from the USLE analysis. The LS factor was grouped into four classes based on existing slope gradient categories, which divided the watershed into six slope classes from flat (0–3%, LS=0.1) to very steep (>40%, LS=11.9). These six classes were combined into four groups relevant to conservation priorities to balance geographical details and management feasibility. The low LS group includes slope classes I-II with a slope of 0–8% and an LS value of 0.1–0.5, representing flat to very gentle topography with minimal erosion risk. The moderate LS group includes slope classes III-IV with a slope of 8–25% and an LS value of 1.4–3.1, representing moderate slopes where agronomic conservation practices are generally adequate. The high LS group includes slope class V with a slope of 25–40% and an LS value of 6.1, which requires mechanical soil conservation structures. Meanwhile, the critical LS group consists of slope class VI with a slope of more than 40% and an LS value of 11.9, which represents very steep slopes where intensive mechanical intervention is necessary to prevent land degradation. This grouping technique maintains physically meaningful slope limits defined in geomorphological literature (e.g., 8% for contour farming feasibility, 25% for terrace requirements, and 40% for critical slope stability), while simplifying the classification for conservation decision-making.

Factor C, which represents vegetation cover and land management conditions, was reclassified into five categories to reflect different levels of soil protection. Unlike the LS factor, which is determined by fixed topography, the C factor is more variable due to differences in the type and intensity of land use management. The classification is based on empirical C values and soil conservation literature guidelines: the Protected class ($C < 0.05$) includes dense natural vegetation such as natural forests ($C = 0.005$) and rice fields ($C = 0.01$); the Good class ($C = 0.05–0.20$) includes production forests ($C = 0.20$) and well-managed annual crop systems; the Moderate class ($C = 0.20–0.50$) includes mixed gardens ($C = 0.50$) and shrublands ($C = 0.30$); Poor class ($C = 0.50–0.90$) represents degraded vegetation or intensive seasonal crop farming; and Critical class ($C > 0.90$) includes residential areas and open land ($C = 1.0$) with very minimal soil protection. A sharper resolution (five classes compared to four for LS) is needed to capture a wider range of vegetation conditions, from virgin forests to completely bare land.

Next, priority zones were determined through spatial tabulation analysis of the reclassified and combined LS and C factors, thereby identifying areas where different combinations of these factors resulted in different priority areas. The LS-C matrix was created as a guide for determining conservation priority order and was validated using Spearman's correlation test between soil loss levels and the established priority rankings. The results of the analysis show a strong monotonically positive relationship between priority ranking and estimated soil loss ($\rho = 0.88$, $p < 0.001$), confirming the validity of the priority matrix. This indicates that the priority classification system effectively distinguishes between levels of erosion severity, with Priority 1 locations experiencing significantly higher soil loss than lower priority classes.

Each spatial combination was then assigned to one of four conservation priority levels using a decision matrix that takes into account the combined severity of the two prominent causes (Table 13). Priority 1 (P1) refers to critical intervention zones with steep topography (LS ≥ High) and inadequate vegetation protection (C ≥ Poor), resulting in a convergence of dominant erosion drivers that require immediate integrated interventions combining mechanical and vegetative measures. Priority 2 (P2) includes high priority zones

Table 12. Results of one-at-a-time sensitivity analysis on USLE parameters

Model Parameters	Value variation range (min – max)	Range of change A (absolute ΔA)	Relative contribution percentage	Dominance level
Rainfall erosivity (R)	1500.38–1232.4	448.90	1.30%	Fourth dominant
Soil erodibility (K)	0.57–0.65	178.75	0.52%	Low
Topography factor (LS)	0,1–11,9	25,728.22	74.70%	Most dominant (1st)
Land cover (C)	0.01–1.0	5,096,53	14.80%	Most dominant (2nd)
Soil conservation (P)	0.15–1.0	2,993.73	8.69%	Third dominant

dominated by a single critical factor—either steep slopes with moderate plant cover or moderate slopes with poor to critical vegetation—that necessitate immediate yet factor-specific actions aimed at the dominating driver. Priority 3 (P3) includes moderate risk zones with balanced factor combinations that necessitate preventive measures rather than intensive interventions, such as steep slopes with good vegetation where forest protection must be maintained, moderate slopes with moderate vegetation suitable for agronomic practices, and flat areas with poor vegetation where gentle topography partially compensates for vegetation deficiency. Priority 4 (P4) addresses low-risk zones where erosion risk is low due to either flat topography regardless of plant condition or any slope with protected vegetation, necessitating simply monitoring to prevent further degradation due to land use change (Figure 10).

After the priority conservation zones have been established, planning efforts can be carried out in each zone using a structured decision-making framework adapted from Fahmuddin and Widianto (2004). This conservation technique selection framework consists of four sequential decision stages that consider the specific characteristics of each priority zone. Stage 1 – identification of dominant factors determines the main erosion factors in each priority zone based on a combination of LS and C, namely: (a) dominated by LS (steep slopes with sufficient vegetation), (b) dominated by C (poor vegetation on moderate slopes), or (c) a combination of LS and C (steep slopes with poor vegetation). Stage 2 – setting control objectives translates dominant factors into specific targets, where LS-dominated zones require reduction of surface flow energy and slope steepness, C-dominated zones require increased infiltration and soil organic matter, while combination zones require simultaneous treatment of both aspects. Stage 3 – approach selection determines general conservation strategies, where LS control uses land cover modification (contour systems, intercropping) or landform modification (terraces, contour ridges), while C control uses organic matter addition (mulch, compost, cover crops) or planting of barrier vegetation and agroforestry. Stage 4 – determination of specific techniques establishes concrete conservation techniques according to local conditions, including mulching and mixed planting for gentle slopes to bench terraces for steep slopes, as well as organic fertilization, crop rotation, and integration of annual crops for long-term protection.

The application of the decision framework at each priority level results in different conservation technique recommendations according to the characteristics of each zone. Priority Zone 1 (dominated by LS and C) requires integrated mechanical and vegetative interventions due to the convergence of steep slopes and poor vegetation. The technical package depends on the severity of the slope: bench terraces with reforestation or agroforestry for very steep slopes (LS = Critical), and contour ridges with vegetation barriers and cover crops for steep slopes (LS = High). The choice between reforestation and agroforestry takes into account land ownership, community economic dependence, and implementation feasibility. Priority Zone 2 (dominated by a single factor) follows the LS or C control path based on the dominant factor. Zones dominated by LS receive mechanical techniques in the form of contour farming systems for moderate slopes and terrace structures for steep slopes while maintaining existing vegetation cover, while zones dominated by C receive vegetative techniques in the form of agroforestry, cover crops, and mulch, with temporary mechanical support (contour intercropping). Priority Zone 3 varies based on specific combinations: protected forests on steep slopes require strict protection and community-based management; moderate slopes with moderate vegetation require agronomic practices such as contour plowing and mulching; flat areas with poor vegetation require vegetation improvement without mechanical structures. Priority Zone 4

Table 13. Priority conservation matrix based on LS and C factor integration

C LS	Protected	Good	Moderate	Poor	Critical
Low	P4	P4	P3	P3	P2
Medium	P4	P3	P3	P2	P1
High	P3	P3	P2	P1	P1
Critical	P2	P2	P1	P1	P1

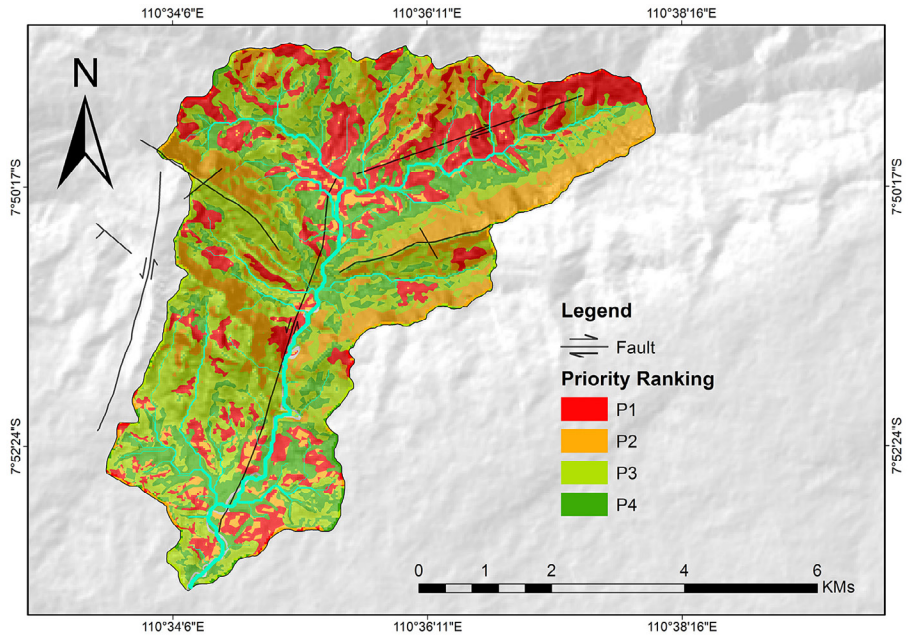

Figure 10. Conservation priority map for the Juwet sub-watershed based on sensitivity analysis of USLE parameters, with four priority classes (P1–P4)

only requires monitoring based on land use to detect early signs of degradation.

Although the decision framework provides a systematic selection of techniques based on dominant factors, the final recommendations take into account three categories of local constraints. First, biophysical constraints include soil depth and texture, which influence terrace design (shallow soil requires stone terraces rather than bench terraces), rainfall intensity patterns, which influence the dimensions of drainage structures, and existing land use, which determines the feasibility of changes in management. Second, socioeconomic constraints include land tenure security, which affects willingness to invest in long-term measures such as terracing; availability of household labor, which affects technical complexity; and market access, which determines the viability of agroforestry products. Third, implementation constraints include the availability of materials (stones for terraces, seedlings for reforestation), technical capacity for construction and maintenance, and community acceptance of the proposed techniques. These constraints were assessed during field validation and community consultations to refine the framework-based recommendations into an implementable conservation plan.

CONCLUSIONS

The potential for erosion in the Juwet sub-watershed shows a strong relationship with topographical characteristics. Areas with the highest potential for erosion are located in the central and upper parts of the sub-watershed, with steep to very steep slopes. Conversely, areas with low potential for erosion are generally found in the downstream alluvial plains with relatively flat topography. The high erosion potential concentrated in steep slope areas correlates with land use in the form of mixed gardens and production forests in these locations, where soil conservation efforts are still minimal. Temporal variations in erosion show a pattern that is consistent with the pattern of rainfall erosivity. The highest erosion potential occurs during the November-March period, which coincides with the rainy season. Conversely, the lowest erosion potential occurs during the May-September period during the dry season. The critical erosion period occurs during the rainy season, especially in November, which contributes the highest erosion potential of 392,324.37 $MJ \cdot mm \cdot ha^{-1} \cdot h^{-1} \cdot month^{-1}$.

Sensitivity analysis of the USLE model identified that topography and land cover were the most dominant parameters, contributing 56.71% and 34.66% respectively to the erosion rate. Building on these findings, a sensitivity-based

conservation planning framework was created by combining the reclassified LS and C factors into a two-factor priority matrix. This approach allows for systematic demarcation of four conservation priority levels (P1–P4), which were statistically confirmed by a high positive association between priority ranking and estimated soil loss ($\rho = 0.88$, $p < 0.001$). The priority classification successfully distinguishes between areas that require immediate integrated actions and those that may be addressed through preventive measures or monitoring.

The suggested land conservation planning framework incorporates scientific findings into a systematic decision-making process that connects main erosion factors to appropriate conservation aims and techniques. While the framework provides a reasonable basis for selecting conservation actions based on biophysical conditions, its implementation should take into account local biophysical, socioeconomic, and institutional restrictions to ensure long-term viability and efficacy. Overall, this study presents a sensitivity-driven approach that can support erosion assessment and conservation prioritization in tropical hilly watersheds with comparable environmental characteristics.

Acknowledgements

The authors would like to thank the Center for Environmental Studies (PSLH), Universitas Gadjah Mada, for providing financial support for this research through a publication grant scheme. Galih Dwi Jayanto, M.Sc., is acknowledged as a co-author affiliated with PSLH. The authors also acknowledge the Serayu Opak River Basin Management Agency (BBWS) for providing rainfall data and the Yogyakarta Agricultural Technology Assessment and Development Agency (BPTP) for soil type data. Furthermore, the authors are grateful to the farmers in Gedangsari, Patuk, and Nglipar subdistricts for their participation in field surveys and assistance during soil sampling.

Funding

This publication of this research was supported by the Center for Environmental Studies at Gadjah Mada University through the PSLH UGM Student Publication Grant 2025 (Contract No. 1246/UN1/PSLH/HK.08.00/2025).

REFERENCES

1. Aldrian, E., Susanto, R. D. (2003). Identification of three dominant rainfall regions within Indonesia and their relationship to sea surface temperature. *International Journal of Clima*, *23*, 1435–1452. https://doi.org/10.1002/joc.950
2. Almagro, A., Thomé, T. C., Colman, C. B., Pereira, R. B., Junior, J. M., Rodrigues, D. B. B., Oliveira, P. T. S. (2019). Improving cover and management factor (C-factor) estimation using remote sensing approaches for tropical regions. *International Soil and Water Conservation Research*, *7*(4), 325–334. https://doi.org/10.1016/j.iswcr.2019.08.005
3. Alves, W. dos S., Martins, A. P., Morais, W. A., Pôssa, É. M., Castro, R. M., Borges de Moura, D. M. (2022). USLE modelling of soil loss in a Brazilian Corrado catchment. *Remote Sensing Applications: Society and Environment*, *27*(100788), 1–19. https://doi.org/10.1016/j.rsase.2022.100788
4. Arsy, R. F. (2008). Pemanfaatan citra ASTER digital untuk estimasi dan pemetaan erosi tanah di daerah aliran Sungai Oyo. *Jurnal Kreatif Tadulako*, *17*(2).
5. Arsyad, S. (2010). *Konservasi tanah dan air* (2nd, Ed.). IPB Press.
6. Assaoui, N. El, Bouiss, C. E., & Sadok, A. (2023). Assessment of water erosion by integrating RUSLE model, GIS and remote sensing – case of Tamdrost Watershed (Morocco). *Ecological Engineering and Environmental Technology*, *24*(3), 43–53. https://doi.org/10.12912/27197050/159530
7. Bahddou, S., Otten, W., Whalley, W. R., Shin, H. C., El Gharous, M., Rickson, R. J. (2023). Changes in soil surface properties under simulated rainfall and the effect of surface roughness on runoff, infiltration and soil loss. *Geoderma*, *431*, 116341. https://doi.org/10.1016/J.GEODERMA.2023.116341
8. Bao, H., Ji, C., Lan, H., Zheng, H., Yan, C., Peng, J., Li, L., Wang, J., Guo, G. (2025). Slope effects on soil moisture migration and evolution in shallow layers of loess high-fill slopes in the Gully Land Consolidation. *CATENA*, *258*, 109206. https://doi.org/10.1016/J.CATENA.2025.109206
9. Ben Cheikha, L., Jaoued, M., Aouadi, T., Ameur, M., Gueddari, M. (2021). Quantifying of water erosion and sediment yield by SEAGIS model in Rmel watershed (north-eastern Tunisia). *Environmental Earth Sciences*, *80*(24), 1–13. https://doi.org/10.1007/s12665-021-10103-z
10. Benzougagh, B., Meshram, S. G., Dridri, A., Boudad, L., Baamar, B., Sadkaoui, D., Khedher, K. M. (2022). Identification of critical watershed at risk of soil erosion using morphometric and geographic information system analysis. *Applied Water Science*, *12*(8), 1–20. https://doi.org/10.1007/s13201-021-01532-z
11. Blanco, H., Lal, R. (2008). *Principles of Soil*

Conservation and Management. Springer International Publishing.

12. Bols, P. (1978). *The Iso-Erodent Map of Java and Madura*.
13. Cahyadi, A., Nurjani, E., Haryono, E., Nugraha, H. (2011). Estimation of soil organic carbon loss by runoff and it's role on management of Ungauge watershed. *Prosiding 3rd International Seminar on Applied Technology, Science and Art, October*.
14. Christanto, N., Setiawan, M. A., Nurkholis, A., Istikhomah, S., Anajib, D. W., Purnomo, A. D. (2019). Rainfall-Runoff and sediment yield modelling in volcanic catchment using SWAT, a case study in Opak Watershed. *IOP Conference Series: Earth and Environmental Science*, *256*(1). https://doi.org/10.1088/1755-1315/256/1/012015
15. Clunes, J., Valle, S., Dörner, J., Martínez, O., Pinochet, D., Zúñiga, F., Blum, W. E. H. (2022). Soil fragility: A concept to ensure a sustainable use of soils. *Ecological Indicators*, *139*, 108969. https://doi.org/10.1016/J.ECOLIND.2022.108969
16. Devatha, C. P., Deshpande, V., Renukaprasad, M. S. (2015). Estimation of soil loss using USLE model for Kulhan Watershed, Chattisgarh- A case study. *Aquatic Procedia*, *4*, 1429–1436. https://doi.org/10.1016/J.AQPRO.2015.02.185
17. Durigon, V. L., Carvalho, D. F., Antunes, M. A. H., Oliveira, P. T. S., Fernandes, M. M. (2014). NDVI time series for monitoring RUSLE cover management factor in a tropical watershed. *International Journal of Remote Sensing*, *35*(2), 441–453. https://doi.org/10.1080/01431161.2013.871081
18. Ewunetu, T., Selassie, Y. G., Molla, E., Admase, H., Gezahegn, A. (2025). Soil properties under different land uses and slope gradients: Implications for sustainable land management in the Tach Karnuary watershed, Northwestern Ethiopia. *Frontiers in Environmental Science*, *13*. https://doi.org/10.3389/fenvs.2025.1518068
19. Fahmuddin, A., Widianto. (2004). *Konservasi Tanah Pertanian Lahan Kering*. World Agroforestry Centre ICRAF Southeast Asia.
20. Farhan, Y., Nawaiseh, S. (2015). Spatial assessment of soil erosion risk using RUSLE and GIS techniques. *Environmental Earth Sciences*, *74*(6), 4649–4669. https://doi.org/10.1007/s12665-015-4430-7
21. Ferro, V., Giordano, G., Iovino, M. (1991). Isoerosivity and erosion risk map for Sicily. *Hydrological Sciences Journal*, *36*(6), 549–564. https://doi.org/10.1080/02626669109492543
22. Feyereisen, G. W., Strickland, T. C., Bosch, D. D., Sullivan, D. G. (2007). Evaluation of SWAT manual calibration sensitivity in the little river watershed. *Transactions of the American Society of Agricultural Engineers*, *50*(3), 843–855. https://doi.org/10.13031/2013.23149
23. Ganasri, B. P., Ramesh, H. (2016). Assessment of soil erosion by RUSLE model using remote sensing and GIS - A case study of Nethravathi Basin. *Geoscience Frontiers*, *7*(6), 953–961. https://doi.org/10.1016/j.gsf.2015.10.007
24. Ge, Y., Zhao, L., Chen, J., Li, X., Li, H., Wang, Z., Ren, Y. (2023). Study on soil erosion driving forces by using (R)USLE framework and machine learning: A case study in Southwest China. *Land*, *12*(3). https://doi.org/10.3390/land12030639
25. Gezici, K., Şengül, S., Kesgin, E. (2025). Assessment of soil erosion risk in the mountainous region of northeastern Türkiye based on the RUSLE model and CMIP6 climate projections. *Environmental Earth Sciences*, *84*(6). https://doi.org/10.1007/s12665-025-12184-6
26. Girmay, G., Moges, A., Muluneh, A. (2020). Estimation of soil loss rate using the USLE model for Agewmariayam Watershed, northern Ethiopia. *Agriculture and Food Security*, *9*(1), 1–12. https://doi.org/10.1186/s40066-020-00262-w
27. Hacisalihoğlu, S., Gümüş, S., Kezik, U., Karadağ, H. (2019). Impact of forest road construction on topsoil erosion and hydro-physical soil properties in a semi-arid mountainous ecosystem in Turkey. *Polish Journal of Environmental Studies*, *28*(1), 113–121. https://doi.org/10.15244/pjoes/81615
28. Hoffland, E., Kuyper, T. W., Comans, R. N. J., Creamer, R. E. (2020). Eco-functionality of organic matter in soils. *Plant and Soil*, *455*(1–2), 1–22. https://doi.org/10.1007/s11104-020-04651-9
29. Javed, A., Khanday, M. Y., Ahmed, R. (2009). Prioritization of sub-watersheds based on morphometric and land use analysis using Remote Sensing and GIS techniques. *Journal of the Indian Society of Remote Sensing*, *37*(2), 261–274. https://doi.org/10.1007/s12524-009-0016-8
30. Jemai, S., Kallel, A., Agoubi, B., Abida, H. (2021). Soil erosion estimation in arid area by USLE model applying GIS and RS: Case of Oued El Hamma Catchment, South-Eastern Tunisia. *Journal of the Indian Society of Remote Sensing*, *49*(6), 1293–1305. https://doi.org/10.1007/s12524-021-01320-x
31. Keesstra, S. D., Bouma, J., Wallinga, J., Tittonell, P., Smith, P., Cerdà, A., Montanarella, L., Quinton, J. N., Pachepsky, Y., Van Der Putten, W. H., Bardgett, R. D., Moolenaar, S., Mol, G., Jansen, B., Fresco, L. O. (2016). The significance of soils and soil science towards realization of the United Nations sustainable development goals. *Soil*, *2*(2), 111–128. https://doi.org/10.5194/soil-2-111-2016
32. Kementerian Kehutanan. (2009). *Tata cara penyusunan rencana teknik rehabilitasi hutan dan lahan daerah aliran sungai (RTkRHL-DAS)*. Kementerian Kehutanan Republik Indonesia.

33. Keshavarzi, A., Kumar, V., Bottega, E. L., Rodrigo-Comino, J. (2019). Determining land management zones using pedo-geomorphological factors in potential degraded regions to achieve land degradation neutrality. *Land*, *8*(6), 1–14. https://doi.org/10.3390/land8060092
34. Koirala, P., Thakuri, S., Joshi, S., Chauhan, R. (2019). Estimation of soil erosion in Nepal using a RUSLE modeling and geospatial tool. *Geosciences (Switzerland)*, *9*(4). https://doi.org/10.3390/geosciences9040147
35. Kuok, K. K. K., Mah, D. Y. S., Chiu, P. C. (2013). Evaluation of C and P factors in universal soil loss equation on trapping sediment: Case study of Santubong River. *Journal of Water Resource and Protection*, *5*(12), 1149–1154. https://doi.org/10.4236/jwarp.2013.512121
36. Lal, R. (1990). *Soil Erosion in the Tropics: Principles and Management*. McGraw-Hill Publishing Company.
37. Luvai, A., Obiero, J., Omuto, C. (2022). Soil loss assessment using the revised universal soil loss equation (RUSLE) model. *Applied and Environmental Soil Science*, *2022*. https://doi.org/10.1155/2022/2122554
38. Mahleb, A., Hadji, R., Zahri, F., Boudjellal, R., Chibani, A., Hamed, Y. (2022). Water-Borne erosion estimation using the revised universal soil loss equation (RUSLE) model over a semiarid watershed: case study of Meskiana Catchment, Algerian-Tunisian Border. *Geotechnical and Geological Engineering*, *40*(8), 4217–4230. https://doi.org/10.1007/s10706-022-02152-3
39. Martins, M. A. S., Ben-Hur, M., Keizer, J. J. (2025). The collapse of recently constructed risers of forest bench terraces and its mitigation. *Geomorphology*, *479*, 109736. https://doi.org/10.1016/J.GEOMORPH.2025.109736
40. Mazigh, N., Taleb, A., El Bilali, A., Ballah, A. (2022). The effect of erosion control practices on the vulnerability of soil degradation in Oued EL Malleh catchment using the USLE model integrated into GIS, Morocco. *Trends in Sciences*, *19*(2). https://doi.org/10.48048/tis.2022.2059
41. Meliho, M., Khattabi, A., Mhammdi, N. (2020). Spatial assessment of soil erosion risk by integrating remote sensing and GIS techniques: a case of Tensift watershed in Morocco. *Environmental Earth Sciences*, *79*(10), 1–19. https://doi.org/10.1007/s12665-020-08955-y
42. Mineo, C., Ridolfi, E., Moccia, B., Russo, F., Napolitano, F. (2019). Assessment of rainfall kinetic-energy-intensity relationships. *Water (Switzerland)*, *11*(10), 1–23. https://doi.org/10.3390/w11101994
43. Oliveira, P. T. S., Rodrigues, D. B. B., Alves Sobrinho, T., Panachuki, E., Wendland, E. (2013). Use of SRTM data to calculate the (R)USLE topographic factor. *Acta Scientiarum – Technology*, *35*(3), 507–513. https://doi.org/10.4025/actascitechnol.v35i3.15792
44. Or, D., Keller, T., Schlesinger, W. H. (2021). Natural and managed soil structure: On the fragile scaffolding for soil functioning. *Soil and Tillage Research*, *208*, 104912. https://doi.org/10.1016/J.STILL.2020.104912
45. Panagos, P., Borrelli, P., Meusburger, K. (2015). A new European slope length and steepness factor (LS-factor) for modeling soil erosion by water. *Geosciences (Switzerland)*, *5*(2), 117–126. https://doi.org/10.3390/geosciences5020117
46. Park, S. J., Burt, T. P. (2002). Identification and characterization of pedogeomorphological processes on a hillslope. *Soil Science Society of America Journal*, *66*(6), 1897–1910. https://doi.org/10.2136/sssaj2002.1897
47. Parveen, R., Kumar, U., Singh, V. K. (2012). Geomorphometric characterization of upper South Koel Basin, Jharkhand: A Remote Sensing & GIS Approach. *Journal of Water Resource and Protection*, *4*(12), 1042–1050. https://doi.org/10.4236/jwarp.2012.412120
48. Pham, T. G., Degener, J., Kappas, M. (2018). Integrated universal soil loss equation (USLE) and geographical information system (GIS) for soil erosion estimation in A Sap basin: Central Vietnam. *International Soil and Water Conservation Research*, *6*(2), 99–110. https://doi.org/10.1016/J.ISWCR.2018.01.001
49. Renard, K. G., Freimund, J. R. (1994). Using monthly precipitation data to estimate the R-factor in the revised USLE. *Journal of Hydrology*, *157*(1–4), 287–306. https://doi.org/10.1016/0022-1694(94)90110-4
50. Saenkang, P., Haq, M. N., Setiawan, H., Wilopo, W. (2024). Landslide susceptibility mapping of Nglipar, Gunungkidul using analytical hierarchy process and geographic information system. *AIP Conference Proceedings*, *3145*(1), 20056. https://doi.org/10.1063/5.0215029
51. Saoud, M., Meddi, M. (2023). Estimation of soil erosion and sediment yield in Wadi El Hachem watershed (Algeria) using the RUSLE-SDR approach. *Journal of Mountain Science*, *20*(2), 367–380. https://doi.org/10.1007/s11629-022-7549-5
52. Satriagasa, M. C., Suryatmojo, H. (2020). Efektivitas Tutupan Rumput Gajah (*Pennisetum purpureum*) dalam Mitigasi Erosi Tanah oleh Air Hujan. *AgriTECH*, *40*(2), 141. https://doi.org/10.22146/agritech.50290
53. Sestras, P., Mircea, S., Roșca, S., Bilașco, Ștefan, Sălăgean, T., Dragomir, L. O., Herbei, M. V., Bruma, S., Sabou, C., Marković, R., Kader, S. (2023). GIS based soil erosion assessment using the USLE model for efficient land management: A case study

in an area with diverse pedogeomorphological and bioclimatic characteristics. *Notulae Botanicae Horti Agrobotanici Cluj-Napoca*, *51*(3), 1–14. https://doi.org/10.15835/nbha51313263

54. Shariffuddin, S. I. M., Udin, W. S. (2020). Landslide susceptibility assessment using geographic information system (GIS) application of Putat Area, Gunungkidul, Yogyakarta, Indonesia. *IOP Conference Series: Earth and Environmental Science*, *596*(1). https://doi.org/10.1088/1755-1315/596/1/012055
55. Shekar, P. R., Mathew, A. (2025). Sub-watershed prioritization for soil erosion: a combined morphometric analysis, PCA, and MCDM approach. *Journal of Engineering and Applied Science*, *72*(1), 1–29. https://doi.org/10.1186/s44147-025-00730-9
56. Srivastava, R. K., Purohit, S., Alam, E., Islam, M. K. (2024). Advancements in soil management: Optimizing crop production through interdisciplinary approaches. *Journal of Agriculture and Food Research*, *18*, 101528. https://doi.org/10.1016/J.JAFR.2024.101528
57. Teku, D., Derbib, T. (2024). Uncovering the drivers, impacts, and urgent solutions to soil erosion in the Ethiopian Highlands: a global perspective on local challenges. *Frontiers in Environmental Science*, *12*(January), 1–19. https://doi.org/10.3389/fenvs.2024.1521611
58. Turner, B. L., Fuhrer, J., Wuellner, M., Menendez, H. M., Dunn, B. H., Gates, R. (2018). Scientific case studies in land-use driven soil erosion in the central United States: Why soil potential and risk concepts should be included in the principles of soil health. *International Soil and Water Conservation Research*, *6*(1), 63–78. https://doi.org/10.1016/J.ISWCR.2017.12.004
59. Ulumia, F., Suprayogi, S., Widyastuti, M. (2025). Estimation of useful life of the Logung Reservoir using universal soil loss equation. *Ecological Engineering and Environmental Technology*, *26*(11), 1–16. https://doi.org/10.12912/27197050/211276
60. Wang, L., Li, Y., Gan, Y., Zhao, L., Qin, W., Ding, L. (2024). Rainfall erosivity index for monitoring global soil erosion. *CATENA*, *234*, 107593. https://doi.org/10.1016/J.CATENA.2023.107593
61. Wischmeier, W. H., Smith, D. D. (1978). *Predicting Rainfall Erosion Losses: A Guide to Conservation Planning (No. 537)*. Department of Agriculture, Science and Education Administration.
62. Yadav, M. B. N., Patil, P. L., Hebbara, M. (2024). Assessment of soil erosion risk in a hilly zone sub-watershed of Karnataka using geospatial technologies and the RUSLE model. *Geology, Ecology, and Landscapes*, *9*(3), 1087–1101. https://doi.org/10.1080/24749508.2024.2373491
63. Yang, M., Yang, Q., Zhang, K., Wang, C., Pang, G., Li, Y. (2023). Effects of soil rock fragment content on the USLE-K factor estimating and its influencing factors. *International Soil and Water Conservation Research*, *11*(2), 263–275. https://doi.org/10.1016/J.ISWCR.2022.07.003
64. Zawiyah, Yanti, D., Irsyad, F., Agita Tjandra, M. (2024). Study of The Erosion Hazard Level (EHL) of Nagari Lawang, Matur District, Agam Regency. *IOP Conference Series: Earth and Environmental Science*, *1426*(1). https://doi.org/10.1088/1755-1315/1426/1/012017
65. Zhang, Z., Yu, R. (2023). Assessment of soil erosion from an ungauged small watershed and its effect on lake Ulansuhai, China. *Land*, *12*(2), 1–15. https://doi.org/10.3390/land12020440